

Design a Multistage Multirate System for Atrial Fibrillation Detection using ECG Signal

By

Fatema Tuj Johura

Roll No. : 1609502

A thesis submitted in partial fulfillment of the requirements for the degree of Master of
Engineering in Electronics and Communication Engineering



Khulna University of Engineering & Technology

Khulna 920300, Bangladesh

November, 2018

Declaration

This is to certify that the thesis work entitled "*Design a Multistage Multirate System for Atrial Fibrillation Detection using ECG Signal*" has been carried out by *Fatema Tuj Johura* in the Department of *Electronics and Communication Engineering*, Khulna University of Engineering & Technology (KUET), Khulna, Bangladesh. The above thesis work or any part of this work has not been submitted anywhere for the award of any degree or diploma.



Signature of Supervisor


Fatema

Signature of Candidate


Approval

This is to certify that the thesis work submitted by *Fatema Tuj Johura* entitled "*Design a Multistage Multirate System for Atrial Fibrillation Detection using ECG Signal*" has been approved by the board of examiners for the partial fulfillment of the requirements for the degree of *Masters of Engineering (M. Sc. Eng.)* in the Department of *Electronics and Communication Engineering*, Khulna University of Engineering & Technology (KUET), Khulna, Bangladesh in November 2018.

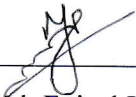
BOARD OF EXAMINERS

1. 

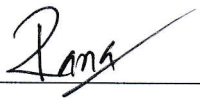
- Dr. Sheikh Md. Rabiul Islam
Professor
Khulna University of Engineering & Technology (KUET)
Khulna, Bangladesh.
- Chairman
(Supervisor)

2. 

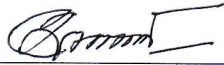
- Dr. A. B. M. Aowlad Hossain
Professor & Head of the Department
Department of Electronics and Communication Engineering
Khulna University of Engineering & Technology (KUET)
Khulna, Bangladesh.
- Member

3. 

- Dr. Md. Foisal Hossain
Professor
Khulna University of Engineering & Technology (KUET)
Khulna, Bangladesh.
- Member

4. 

- Dr. Md. Masud Rana
Associate Professor
Khulna University of Engineering & Technology (KUET)
Khulna, Bangladesh.
- Member

5. 

- Dr. Mirza A. F. M. Rashidul Hasan
Professor
Dept. of Information and Communication Engineering (ICE)
University of Rajshahi
Rajshahi-6205, Bangladesh.
- Member
(External)

Acknowledgements

First of all, I would like to bend myself to Almighty for giving me the strength and confidence to complete my thesis work, successfully.

Then I would like to acknowledge my deep gratitude to my graduation committee.

*It is a great pleasure to express my deepest gratitude and profound respect to my honorable supervisor, **Dr. Sheikh Md. Rabiul Islam**, Professor, Department of Electronics and Communication Engineering, KUET, who fully gave many invaluable advices, proper guidance, constant encouragement, constructive suggestions kind co-operation throughout The entire progress of this thesis work.*

I wish to complement to all teachers of the Department of Electronics and Communication Engineering, KUET for their co-operations and relentless encouragements in various ways throughout this work.

Finally, it is my duty to express gratefulness and appreciations to my family members for their unswerving inspirations to complete my work.

Fatema Tuj Johura
November, 2018

Abstract

Atrial Fibrillation (AF) is one of the most common cardiac arrhythmias. The number of patients related to heart failure due to AF is increasing day by day. Early detection of AF may reduce the risk of death due to heart failure. So, it has become more important to detect AF. There are various methods to detect AF. In this thesis, we use ECG signal for AF detection. The MIT-BIH Atrial Fibrillation database is used to import ECG data for analysis. Filtered ECG signal using multistage multirate system for removing noise. RR interval of the ECG signal is calculated. Here we use the algorithm that mainly follows statistical method for detection of AF. Parametric statistics RMSSD and SE, and non-parametric statistics, TPR are used for this purpose. MATLAB R2016a is used to measure the values of those parameters for estimation of AF. The threshold values of RMSSD/ (Mean RR) taken from the literature is 0.1, SE is 0.7 and TPR is greater than 0.54 and lesser than 0.77. The resultant values of RMSSD, SE and TPR of every beat are checked whether it crosses the threshold level or not. If all the three parameters cross the threshold level then the beat is flagged as AF. It shows excellent results when compared with the annotations of the database, and then the sensitivity, specificity and accuracy are determined. The algorithm has a sensitivity of 98.03%, specificity of 98.80% and accuracy of 99.45%. Thus, the results obtained in this study are appreciable compared to other studies found in literature.

Thesis Contribution

1. **Fatema tuj Johura, Sheikh Md. Rabiul Islam, “Novel Multistage Multirate system for ECG signal”, *International Journal of Electronics and Communication Engineering*, vol. 7, issue 2, pp. 23-34, March 31, 2018.**
2. **Fatema tuj Johura, Sheikh Md. Rabiul Islam, Md. Maniruzzaman, Mahdi Hasan, “ECG Signal for Atrial Fibrillation Detection”, *2017 International Conference on Electrical, Computer & Communication Engineering (ECCE2017)*, *IEEE explore*, Cox Bazer, Bangladesh, pp.928-934, 16-18 Feb. 2017.**

Contents

	Page
Title Page	i
Declaration	ii
Approval	iii
Acknowledgement	iv
Thesis Contribution	v
Abstract	vi
Contents	vii
List of Tables	x
List of Figures	xi
List of Abbreviations	xiv
CHAPTER I Introduction	1-10
1.1 Introduction	2
1.2 Motivation	2
1.3 Problem Statement	4
1.3.1 Some Risk Factors Experienced by AF Patients	5
1.3.2 Hospitalization Due to AF	5
1.3.3 AF-Related Hospital Discharges	7
1.3.4 Economic Burden of AF	7
1.4 Objectives	8
1.5 Organization of Thesis	8
<i>References</i>	10
CHAPTER II Background and Related Work	11-39
2.1 Introduction	12
2.2 Electrocardiography	12
2.2.1 When an ECG is Used	14
2.2.2 Types of ECG	15
2.2.3 Different ECG Waves	15
2.2.4 The Electric Discharge of the Heart	18
2.3 Overview of Basic Noises in ECG Signal	19

2.3.1	Power-line Interference Noise (PLI)	20
2.3.2	Electrode Contact Noise	21
2.3.3	Motion Artifact	21
2.3.4	Electromyography Noise (EMG)	22
2.3.5	Baseline Wander	22
2.3.6	Burst Noises	22
2.3.7	Instrumentation Noise	23
2.4	Filtering	23
2.5	Multirate System	24
2.6	Multistage Systems	25
2.7	Atrial Fibrillation	26
2.8	The Heart in Normal	26
2.9	The Heart During AF	28
2.10	Diagnosis and Treatment - Challenges in AF	28
2.11	ECG Signal for AF Detection	29
2.12	History of AF Detection	30
2.12.1	Diagnostic Testing	31
2.12.2	Biological Imaging	31
2.12.3	Statistical Analysis	32
2.12.4	Electrocardiography	32
2.12.5	Echocardiography	32
2.12.6	Transesophageal Echocardiography	32
2.12.7	Chest X-ray	32
2.13	Review of Related Research Work on Thesis	33
2.13.1	RR Irregularity (RRI)	34
2.13.2	Atrial Activity (AA)	34
2.13.3	Combination of RRI and AA	34
2.14	Summary	35
	<i>References</i>	36
CHAPTER III	Multistage Multirate System	40-63
3.1	Introduction	41
3.2	Materials and Methods	41
3.2.1	Database	41

3.2.2	FIR Filter Design	43
3.2.3	Polyphase Decomposition	43
3.2.4	Proposed Multistage Multirate Polyphase Filter	45
3.3	Results and Discussion	55
3.4	Summary	61
	<i>References</i>	62
CHAPTER IV	Atrial Fibrillation Detection	64-85
4.1	Introduction	65
4.2	Materials and Methods	66
4.2.1	Database	66
4.2.2	Software and Proposed Algorithm	66
4.2.3	Detection Methods	69
4.2.4	Performance Criteria	72
4.3	Results and Discussion	72
4.3.1	Import of ECG Signal	72
4.3.2	Filtering of Baseline Noise of ECG Signal	73
4.3.3	R-R Peak Detection	74
4.3.4	Signal for RR Peak Differences	75
4.3.5	AF Detection Results	76
4.3.6	Performance Analysis of Proposed Algorithm	79
4.4	Summary	83
	<i>References</i>	84
CHAPTER V	Conclusion and Future Work	86-87
5.1	Conclusion	87
5.2	Future work	87

LIST OF TABLES

Table No	Description	Page
1.1	Burden of AF in comparison with the total burden of CV conditions in Scotland	6
3.1	List of original ECG signals taken from MIT-BIH Atrial Fibrillation Database	42
3.2	The impulse response $h(n)$ or filter coefficients of frequency sampling filter (N=9)	47
3.3	The impulse response $h(n)$ or filter coefficients frequency sampling filter (N=81)	50
4.1	Threshold levels of 15 original ECG signals recorded in MIT-BIH Atrial Fibrillation database	75
4.2	Number of NSR and AF detected in our algorithm	78
4.3	Number of TP, TN, FP and FN for each ECG signal	80
4.4	The calculated value of sensitivity, specificity and accuracy of the tested data	81
4.5	The weighted value of sensitivity, specificity and accuracy of the tested data	82

LIST OF FIGURES

Figure No	Description	Page
1. 1	AF related hospital activity by age of patient in Scotland in 2008	7
2. 1	A General ECG waveform with P, Q, R, S, T and U peak	13
2. 2	A General ECG waveform with normal value of intervals.	14
2. 3	P-waves in ECG signal	15
2. 4	QRS complex in ECG signal	16
2. 5	T-waves in ECG signal	17
2. 6	U-waves in ECG signal	18
2. 7	The conduction system of the heart	19
2. 8	ECG signal + power line Interference	20
2. 9	Multistage implementation of decimator	25
2. 10	Multistage implementation of interpolator	25
2. 11	The single-stage equivalence for the multistage structure of Figure 2.9	25
2. 12	The single stage equivalence for the multistage structure of Figure 2.11	26
2. 13	Anatomy of the heart	27
2. 14	Different parts of the ECG signal during NSR	29
2. 15	Examples of ECG signals during (a) NSR and (b) AF and (c) both NSR and AF	30
3. 1	Commutative polyphase structure of an interpolator	44
3. 2	Commutative polyphase structure of a decimator	45

Figure No	Description	Page
3. 3	Proposed diagrams for multistage implementation of sampling rate alteration system	46
3. 4	Frequency response of design low pass for FIR filter	47
3. 5	Proposed multistage multirate system for case I	48
3. 6	Frequency response of design low pass for FIR filter	51
3. 7	Proposed multistage multirate system for case II	52
3. 8	Proposed multistage multirate system for case III	55
3. 9	Multistage filtering of noisy ECG signal (MIT BIH AF 08215m.mat) for case I	56
3. 10	(a) Multistage filtering of noisy ECG signal (MIT BIH AF 08215m.mat) zoom in part & Frequency response (b) Normalized Autocorrelation for Case I	57
3.11	Multistage filtering of noisy ECG signal (MIT BIH AF 08215m.mat) for case II	57
3. 12	(a)Multistage filtering of noisy ECG signal (MIT BIH AF 08215m.mat) zoom in part & Frequency response (b) Normalized Autocorrelation for Case II	58
3.13	Multistage filtering of noisy ECG signal (MIT BIH AF 08215m.mat) for case III	59
3. 14	(a) Multistage filtering of noisy ECG signal(MIT BIH AF 08215m.mat) Zoom in part & Frequency distribution by histogram (b) Normalized Autocorrelation for Case III	60

Figure No	Description	Page
4. 1	Our proposed algorithm, which shows the total process of detecting AF	68
4. 2	Time domain representation of original ECG signal (File # 04048)	73
4. 3	Time domain representation of filtered ECG (File # 04048)	74
4. 4	R peak detection of the filtered ECG signal (File # 04048)	74
4. 5	Wave shapes of RR interval of the signal (File # 04048)	76
4. 6	Result of RMSSD of the signal (File #04048)	76
4. 7	Result of SE of the signal (File #04048)	77
4. 8	Result of TPR of the signal (File #04048)	77

LIST OF ABBREVIATIONS

Abbreviated Form	Elaboration
AA	Atrial Activity
AF	Atrial Fibrillation
AFL	Atrial Flutter
AV	Atrioventricular
CV	Cardiovascular
FIR	Finite impulse response
FN	False Negative
ECG	Electrocardiogram
FP	False Positive
FSA	Frequency Spectrum Analysis
HRV	Heart Rate Variability
IFFT	Inverse Fast Fourier Transform
MATLAB	Matrix Laboratory
MM	Markov Model
NN	Neural Network
NSR	Normal Sinus Rhythm
PWA	P Wave Absence
RMSSD	Root Mean Square of Successive Differences
RRI	R-peak to R-peak Interval
SA	Sinoatrial
SE	Shannon Entropy
Se	Sensitivity
Sp	Specificity
PPV	Positive Predictive Value
TN	True Negative
TP	True Positive
TPR	Turning Point Ratio

CHAPTER I

Introduction

Chapter Outlines

- Introduction
- Motivation
- Problem Statement
- Objectives
- References

CHAPTER I

Introduction

1.1 Introduction

Biomedical signals are described as the collection of electrical signals acquired from any organ that represents a physical variable of interest. These signals are normally a function of time. They are described in terms of their amplitude, frequency and phase. The analysis of these signals is important both for research and for medical diagnosis and treatment. If the signals are not properly diagnosed and analyzed, it will lead to wrong diagnosis and can be fatal to life. Biomedical signals such as ECG, EMG, EEG and EOG -are extremely important in the diagnosis of patients. These signals have noise as well as artifacts which have to be removed for proper treatment of a patient. Different methodologies have been used to remove noise and artifacts from ECG signals and detecting AF using ECG signal which is the goal of this thesis.

1.2 Motivation

Today, heart disease and related faults are among the leading causes of death in the world. Therefore, it is necessary to have an appropriate method that determines the patient's heart condition. The ECG inspection is one of the methods. Electrocardiography (ECG) is a tool used to understand the condition of the heart. The ECG records the electrical signals (activity) that are generated throughout the cardiac cycle through electrodes placed in various places on the surface of the body. A patient's ECG is visually examined in the time domain. But this ECG is full of noise that can be reduced by processing the signal. Signal processing is an important and obvious tool in the fields of biomedical engineering. Today, the flow of biomedical signal processing has advanced to the stage of practical application of signal processing techniques and pattern analysis. The ECG signal is a graphic representation of cardiac activity and is used to investigate various abnormalities that are present in the heart. Typically, an ECG signal consists of P wave, QRS complex, T wave and any deviation in these parameters predicts and justifies the anomalies present in the heart. The electrocardiogram (ECG) signals are usually contaminated by baseline deviation (BW).

Changes in skin impedance of the electrodes due to perspiration, patient movement and respiration, which contributes to the deviation of the baseline. Computer-based processing is influenced due to the deviation of the baseline. Noise reduction, such as BW and power interference, is a necessity, so the ECG signal can be analyzed automatically by a computer and finally interpreted by a cardiologist. The elimination of various disturbances is one of the first steps in the processing of the ECG, not only before the additional automatic processing, but also as a first step in the visual diagnosis. The purpose of this diagnosis is to facilitate processing and allow reliable measurements of the ST segment. The ambulatory ECG records that are taken when the electrodes are placed in the subject's chest are contaminated by different types of artifacts. The ECG artifacts are the perturbations in the ECG, which is a measure of the cardiac potentials in the human body. Normal components of the ECG can be distorted due to artifacts. Artifacts are quite common and adequate knowledge is necessary to avoid misinterpretation of the patient's ECG. Artifacts can be generated due to electrical interference from the external source, electrical noise in other parts of the body, poor contact and malfunction of the machine. The positive stress ECG test indicates that the QRS complex is modified as it increases and patients may have significant coronary artery disease.

Noisy ECG signals contain variations in the amplitudes or time intervals that represent anomalies associated with the heart; This makes it difficult to diagnose cardiovascular diseases. Therefore, to facilitate the proper analysis of ECG; This document presents a combination of wavelet analysis and morphological filtering as an approach for the elimination of noise in ECG signals. The proposed algorithm involves the decomposition of sub-bands of the ECG signal using a family of bi-orthogonal wavelets. The wavelet detail coefficients that contain the noisy components are processed by morphological operators using elements of linear structuring. The morphological filter processes only the damaged bands without affecting the parameters of the signal. The results of the simulation of the proposed algorithm show a remarkable suppression of noise in terms of a higher signal-to-noise ratio that preserves the ST segment and the R wave of the ECG.

Heart disease is one of the leading causes of death worldwide. He is an equal opportunity killer who claims millions of lives annually. Doctors use the electrocardiogram (ECG) to detect abnormal heart rhythms and investigate the cause of chest pain. This test detects and records the electrical activity of the heart. An ECG is nothing more than a record of the strength and timing information of electrical signals as they pass through the heart.

A common problem in the interpretation of the ECG is the elimination of unwanted artifacts and noises. There are several artifacts that are added to these signals and change the original signal, therefore, the need to eliminate these artifacts from the original signal is significant. An ECG signal consists of very low frequency signals of approximately 0.5 Hz-100Hz and the digital filters are very efficient to eliminate the noise of such low frequency signals. Cardiac monitors are devices that provide a means to filter ECG recording. The noise filtering methods have a decisive influence on the performance of all ECG signal processing systems. This thesis aims to review different sources of noise associated with the acquisition and processing of ECG signals, together with a brief study of several multirate multistage systems implemented to reduce it. Finally, detect AF using filtered ECG signal.

Among the heart diseases, AF is the most common cardiac arrhythmia found in clinical practice with increased prevalence in the ageing population [1.1]. It affects 5% of those aged over 65 years and 10% of those aged over 80 years [1.1]. Its prevalence is increasing primarily for two reasons; an increase in the ageing population and advances in medical care leading to survival from underlying conditions closely associated with AF, such as hypertension, coronary heart disease, and cardiac failure [1.1]. Because of those conditions, AF has come with an increased rate of hospitalizations and medical care. It also has a huge economic impact. It has been described as epidemic in proportion since some researchers have predicted its prevalence will triple by 2050 [1.1]. So, if the AF is detected early then it could reduce the cost of treatment, rate of hospitalization and other risk factor associating with it.

1.3 Problem Statement

In previous years, many different techniques are used for removing noise from ECG signals to detect AF using ECG signals. The methods were based on adaptive filtering, average filtering, adaptive neuro-fuzzy inference system (ANFIS), wavelet transform, least mean squares (LMS), normalized least mean squares (NLMS), least mean Mestimate (LMM), normalized least mean Mestimate (NLMM), mathematical morphology filtering method and so on. Each of these methods have limitations. In this thesis, a new technique of filtering the ECG signals which is based on multirate filtering scheme has been proposed to overcome that limitations. For removing noise from ECG signal three different algorithms based on multistage multirate systems will be proposed and described in chapter IV.

The goal of this thesis is to achieve better filtered signal with removing noise as much as can then detecting AF using filtered ECG signal. Proper diagnosis is essential for proper treatment. There are also various methods to detect AF, such as, Electrocardiography (ECG), Echocardiography, Transesophageal Echocardiography, and Chest X-Ray. However, AF is usually diagnosed from the surface ECG to conform its presence.

Today, there is no clinical test available that can predict the natural history of AF and the outcome of treatment. Since an ECG is recorded from practically all AF patients, it is desirable to classify AF from the ECG signal, to help physicians in deciding which treatment is appropriate for a specific patient. The characteristics of the ECG signal during AF varies not only between different patients, but also in the same patient over time. One important challenge is to track such changes in long term ECG recordings which usually are recorded during ambulatory conditions.

1.3.1 Some Risk Factors Experienced by AF Patients

More than one-third of patients who experience a stroke return to their home with some level of permanent disability [1.2]. They then rely on informal care, typically from family members, to help with their normal daily activities and to arrange the required additional assistance from healthcare services. The disabling consequences of stroke are worse for those patients who survive an AF related stroke, than for those without AF. The presence of AF increases the risk of remaining disabled after a stroke by almost 50% [1.3].

1.3.2 Hospitalization Due to AF

From a study period from 2004 to 2008, a total of 162,449 hospital episodes in Scotland were coded with a primary or a secondary diagnosis of AF, as shown in Table 1.1.

Table 1. 1: Burden of AF in comparison with the total burden of CV conditions in Scotland [1.1].

Year	Hospital inpatient episodes		Hospital treated patients		Hospital discharges*		Inpatient bed days	
	AF patients	CV patients	AF patients	CV patients	AF patients	CV patients	AF patients	CV patients
2004	28613	147,566	21,907	102,552	41,085	208,602	344,164	1,458,203
2005	30410	158,959	22,942	109,124	44,573	224,971	364,419	1,508,261
2006	32551	167995	24,264	114,540	47,205	235,637	390,256	1,561,310
2007	34671	173,636	25,472	117,431	51,631	246,630	402,229	1,549,716
2008	36204	173,704	26,510	117,343	54,686	251,052	394,128	1,515,705
*includes inpatient and outpatient discharges and death								

There were 28,613 hospital episodes (20.0 per 1,000 population) in 2004, which increased to 36,204 by 2008 (24.2 per 1,000 population); representing a 26.5% increase over the five-year study period (Table 1.1). Throughout this period, cumulatively, men accounted for more hospital episodes than women (120.1/1,000 compared with 99.5/1,000). The number of AF-related hospital episodes increased from 14,284 in women.

There were 147,566 hospitalizations related to cardiovascular (CV) conditions in 2004 (103.2 per 1,000 population) increasing to 173,704 (116.3 per 1,000 population) in 2008, which represents a 17.7% increase in five years, in contrast to the 26.5% increase for AF hospitalization during the same period [1.1]. Of the total CV hospitalizations, those related to AF increased from 19.4% in 2004 to 20.8% in 2008, indicating a rising contribution of AF to total CV hospitalization, as displayed in Table 1.1.

1.3.3 AF Related Hospital Discharges:

Total AF-related discharges, which included inpatient and day-case discharges, as well as deaths, increased by 33.1% during the study period from 2004 to 2008 compared with an overall increase of 20.4% in CV patients, as displayed in Table 1. The population standardized estimates indicated 28.7 discharges per 1,000 in 2004 increasing to 36.6 discharges per 1,000 in 2008. AF accounted for approximately 19.7% of cardiovascular discharges in 2004, which increased to approximately 21.8% in 2008, suggesting an overall increase in AF-related hospitalizations in Scotland during this period [1.1]. The five-year cumulative hospital discharges were higher among men (172.8/1,000 population) compared with women (149.6/1,000 population) [1.1]. The total discharges attributable to AF increased steadily with age such that patients aged 55–59 years had 6.8 discharges per 1,000, increasing to 129.5 discharges per 1,000 among patients 85 years and over in 2008. The overall AF-related activity by age of patients in 2008 is displayed in Fig. 1.1.

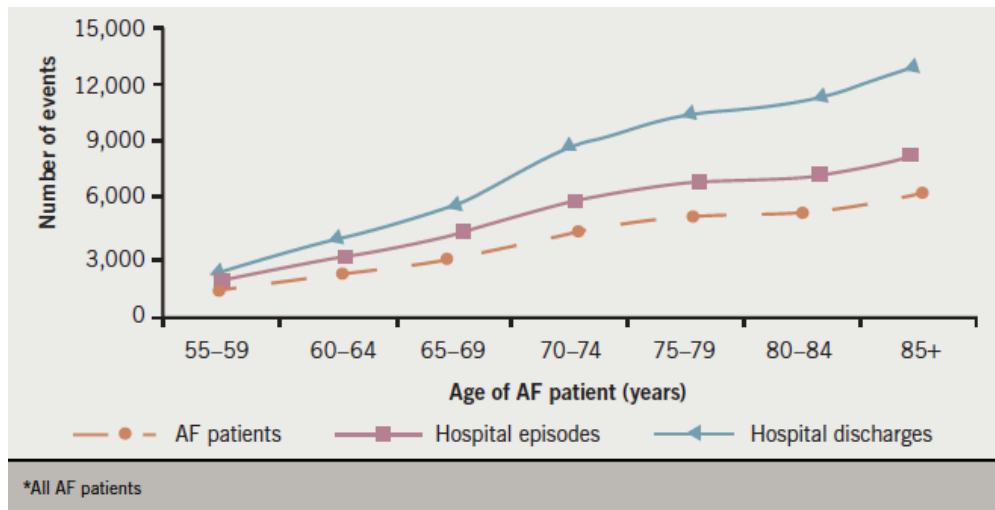


Figure 1. 1: AF related hospital activity by age of patient in Scotland in 2008 [1.1].

1.3.4 Economic Burden of AF

The total cost for CV inpatients in Scotland increased from £622.9 million in 2004 to £655.5 million in 2008 [1.1]. The total inpatient cost of AF also increased from £136.4 million in 2004 to £159.3 million in 2008 [1.1]. The inpatient cost per patient, however, decreased for both cardiovascular (£6,074.0 per cardiovascular patient in 2004 to £5,586.2 per

cardiovascular patient in 2008) and AF patients (£6,226.3 per AF patient in 2004 to £6,009.0 per AF patient in 2008) [1.1]. The average inpatient costs for AF were 16.7% more in women (£6,719.5 per patient) than men (£5,756.4 per patient) over the five-year study period [1.1]. So, it is clearly seen from the statistics above that AF has an increased rate of hospitalization and cost from day by day. Proper steps should be taken for early detection of AF to decrease those rates.

1.4 Objectives

The major objectives of this research are as follows:

- (i) To design multistage multirate filter structure with different cases. The structure will be composed of multistage analysis and synthesis filter.
- (ii) Detection of Atrial Fibrillation (AF) using ECG signal after filtering by multistage Multirate System.
- (iii) To find out RR interval of ECG signal by root mean squares of successive differences (RMSSD), sample entropy, Shannon entropy (SE), turning point ratio (TPR) values.
- (iv) To verify the performance of the obtained results of AF detection in terms of sensitivity (Se), specificity (Sp), accuracy.

1.5 Organization of Thesis

This section provides a summary of the all the chapters covered in this thesis.

Chapter-I:

This chapter gives the introduction of the thesis, the motivation, the problem description, objective and also detail of report layout of the thesis report.

Chapter-II:

This chapter gives the basic knowledge of ECG and its history. Here types of ECG, different waves of ECG such as P, U, QRS complex, T waves and their descriptions are described. Different types of noises which affects the ECG signal then multistage multirate filtering systems. It also gives the basic knowledge of Atrial Fibrillation (AF), diagnosis and treatment- challenges in AF, ECG signal for AF detection, history of AF detection and previous related works are also described.

Chapter-III:

This chapter presents the brief description of three multistage multirate systems which are to be employed in this thesis to perform the noise cancellation. It also gives the overview of the process and operations of systems.

Chapter-IV:

This chapters gives the overview of the total process of AF detection using ECG signal.

Chapter-V:

This chapter will provide the conclusion and future research. It also gives the detail of the thesis goal, its achievement and what has been concluded after completion this thesis.

REFERENCES

- [1.1] M. Keech, Y. Punekar, A. M. Choy, “Trends in Atrial Fibrillation Hospitalisation in Scotland”, *An Increasing Cost Burden, Br. J. Cardiol*, vol.19, pp. 173–177, 2012.
- [1.2] J. Slocum, E. Byrom, L. M. Carthy, A. Sahakian and S. Swiryn, “Computer Detection of Atrioventricular Dissociation from Surface Electrocardiograms during Wide QRS Complex Tachycardia”, *Circ.*, vol. 72, pp. 1028–1036, 1985.
- [1.3] R. L. Streit and R. F. Barrett, “Frequency line tracking using hidden Markov models”, in *IEEE Transactions on Acoustics, Speech, and Signal Processing*, vol. 38, no. 4, pp. 586-598, April 1990.

CHAPTER II

Background and Related Work

Chapter Outlines

- Introduction
- Electrocardiography
- Overview of Basic Noises in ECG Signal
- Filtering
- Multirate System
- Multistage System
- Atrial Fibrillation
- The Heart in Normal
- The Heart During AF
- Diagnosis and Treatment - Challenges in AF
- ECG Signal for AF Detection
- History of AF Detection
- Review of Related Research Work on Thesis
- Summary
- References

CHAPTER II

Background and Related Work

2.1 Introduction

For analyzing of ECG signal, it is important to understand the physiology of ECG. In this chapter, at first a brief introduction of ECG is given. Then a detail discussion on various noises in ECG signal will be given. After that filtering using multistage multirate systems. Finally, Atrial Fibrillation and effects will be discussed.

2.2 Electrocardiography

Electrocardiography is a process used to record electrical activities of the heart over a period of time using electrodes placed on a patient's body. These electrodes detect the tiny electrical changes on the skin that arise from the heart muscle's electrophysiological pattern of depolarizing and repolarizing during each heartbeat. It is a very commonly performed cardiology test.

Electrocardiography is the process of recording of electrical activity of the heart. An electrocardiogram — abbreviated as EKG or ECG — is a test that measures the electrical activity of the heartbeat. With each beat, an electrical impulse (or “wave”) travels through the heart. This wave causes the muscle to squeeze and pump blood from the heart. A normal heartbeat on ECG will show the timing of the top and lower chambers [2.1].

The right and left atria or upper chambers make the first wave called a “P wave” — following a flat line when the electrical impulse goes to the bottom chambers. The right and left bottom chambers or ventricles make the next wave called a “QRS complex.” The final wave or “T wave” represents electrical recovery or return to a resting state for the ventricles [2.2]. The different peaks P, Q, R, S, T, and U are noticeable at these stages, as observed in Figure 2.1. If ECG is properly analyzed, can provide us information regarding various diseases related to heart. Moreover, visual analysis cannot be relied upon. This calls for computer-based techniques for ECG analysis [2.1].

An ECG gives two major kinds of information. First, by measuring time intervals on the ECG, a doctor can determine how long the electrical wave takes to pass through the heart.

Finding out how long a wave takes to travel from one part of the heart to the next shows if the electrical activity is normal or slow, fast or irregular. Second, by measuring the amount of electrical activity passing through the heart muscle, a cardiologist may be able to find out if parts of the heart are too large or are overworked [2.1].

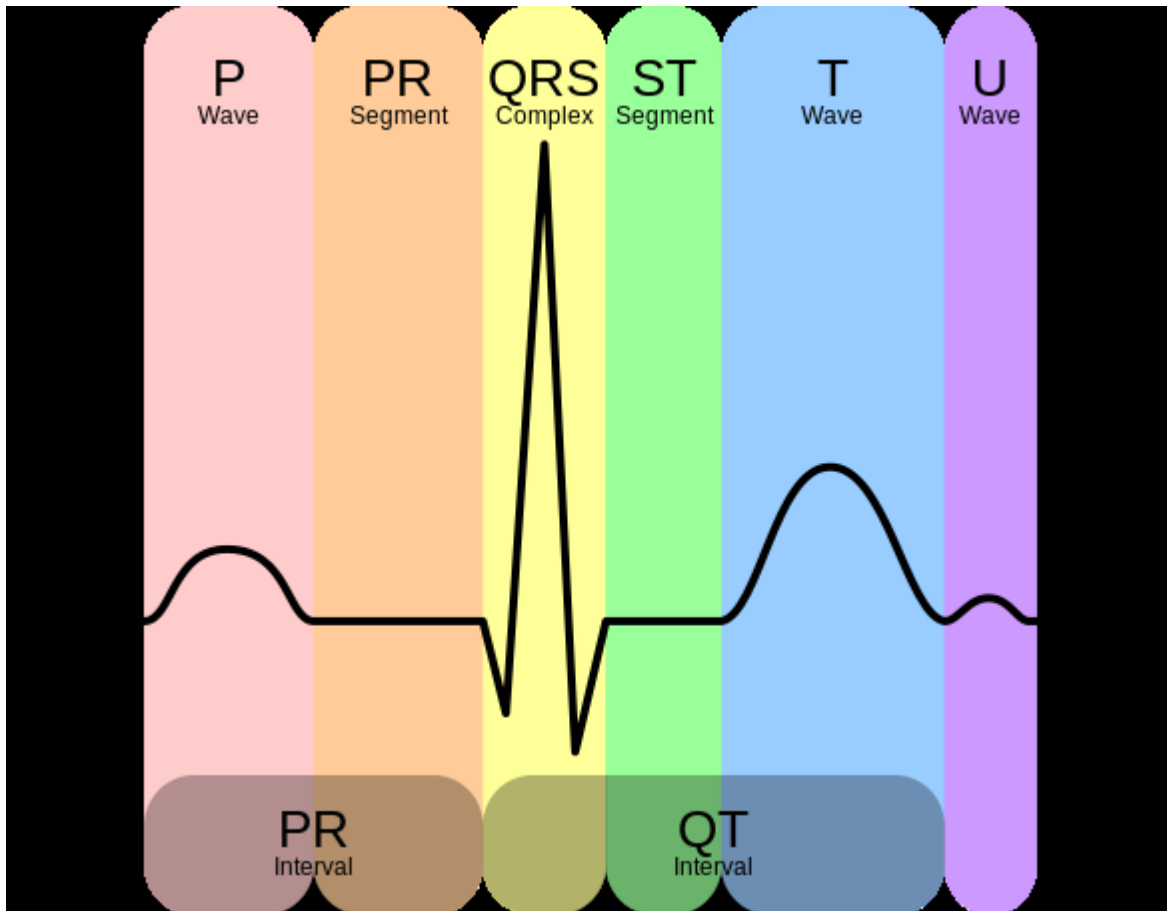


Figure 2. 1: A General ECG waveform with P, Q, R, S, T and U peak [2.2].

Figure 2.2 shows the standard ECG waveform along with intervals the normal value of the parameters.

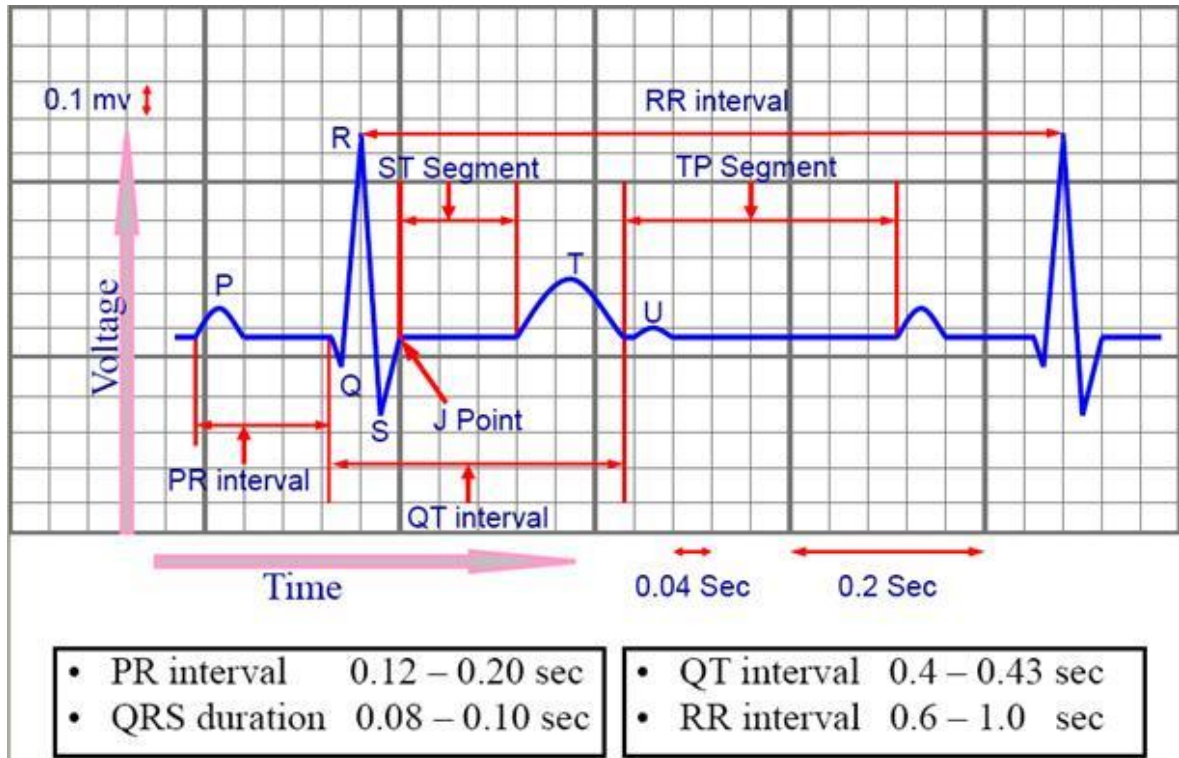


Figure 2. 2: A General ECG waveform with normal value of intervals [2.2].

2.2.1 When an ECG is Used

An ECG is often used alongside other tests to help diagnose and monitor conditions affecting the heart. It can be used to investigate symptoms of a possible heart problem, such as chest pain, suddenly noticeable heartbeats (palpitations), dizziness and shortness of breath [2.1], [2.2], [2.3].

An ECG can help detect:

- Arrhythmias – where the heart beats too slowly, too quickly, or irregularly.
- Coronary heart disease – where the heart's blood supply is blocked or interrupted by a build-up of fatty substances.
- Heart attacks – where the supply of blood to the heart is suddenly blocked.
- Cardiomyopathy – where the heart walls become thickened or enlarged.

A series of ECGs can also be taken over time to monitor a person already diagnosed with a heart condition or taking medication known to potentially affect the heart.

2.2.2 Types of ECG

There are three main types of ECG.

- a resting ECG – carried out while you're lying down in a comfortable position
- a stress or exercise ECG – carried out while you're using an exercise bike or treadmill
- an ambulatory ECG – the electrodes are connected to a small portable machine worn at your waist so your heart can be monitored at home for one or more days

The type of ECG recommended for you will depend on your symptoms and the heart problem suspected. For example, an exercise ECG may be recommended if your symptoms are triggered by physical activity, whereas an ambulatory ECG may be more suitable if your symptoms are unpredictable and occur in random, short episodes [2.1].

2.2.3 Different ECG Waves

P Wave

- The P wave is the first positive deflection on the ECG
- It represents atrial depolarization

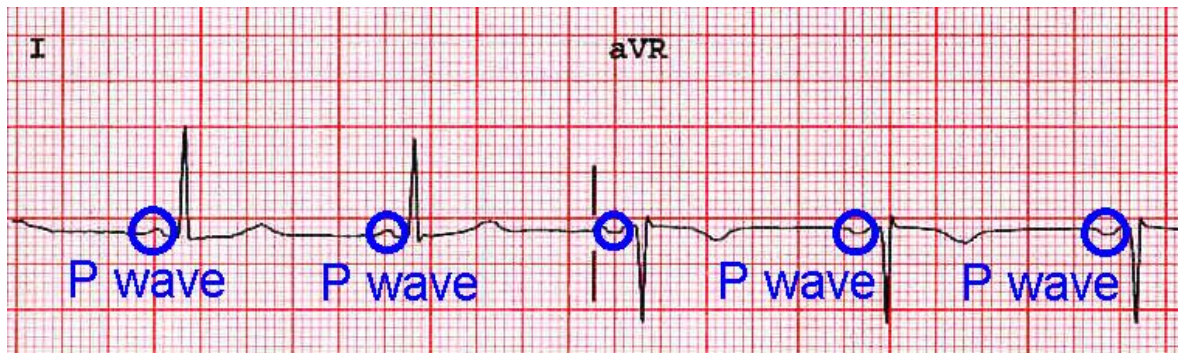


Figure 2. 3: P-waves in ECG signal [2.2].

Morphology

- Smooth contour
- Monophasic in lead II
- Biphasic in V1

Axis

- Normal P wave axis is between 0° and $+75^\circ$
- P waves should be upright in leads I and II, inverted in aVR

Duration

- < 120 ms
- Amplitude
- < 2.5 mm in the limb leads,
- < 1.5 mm in the precordial leads

QRS Complex

The QRS complex represents the rapid depolarization of the right and left ventricles. The ventricles have a large muscle mass compared to the atria, so the QRS complex usually has a much larger amplitude than the P-wave.

If the QRS complex is wide (longer than 120 ms) it suggests disruption of the heart's conduction system, such as in Left bundle branch block (LBBB), Right bundle branch block (RBBB), or ventricular rhythms such as ventricular tachycardia.

Metabolic issues such as severe hyperkalemia, or TCA overdose can also widen the QRS complex. An unusually tall QRS complex may represent left ventricular hypertrophy while a very low-amplitude QRS complex may represent a pericardial effusion or infiltrative myocardial disease [2.1].

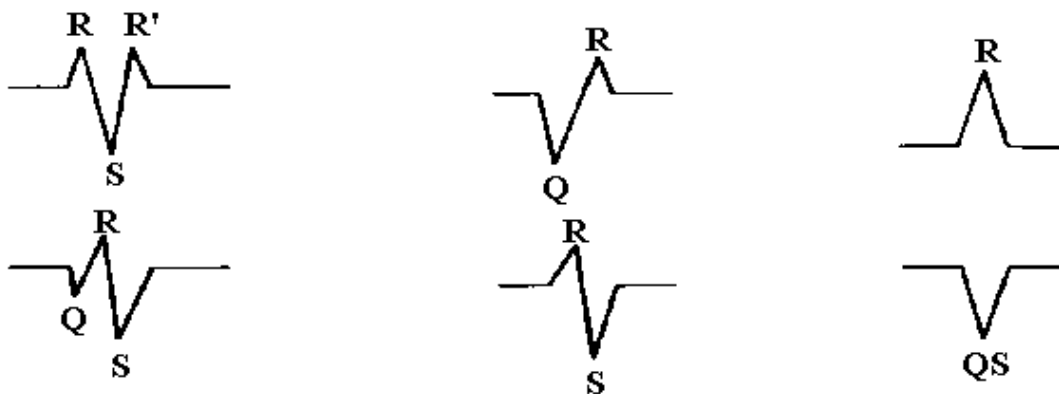


Figure 2. 4: QRS complex in ECG signal [2.2].

T Wave

- The T wave is the positive deflection after each QRS complex
- It represents ventricular repolarization
- Upright in all leads except aVR and V1
- Amplitude < 5mm in limb leads, < 15mm in precordial leads

- Duration 160ms



Figure 2. 5: T-waves in ECG signal [2.2].

U Wave

The U wave is a small (0.5 mm) deflection immediately following the T wave, usually in the same direction as the T wave. It is best seen in leads V2 and V3. The source of the U wave is unknown. Three common theories regarding its origin are:

- Delayed repolarization of Purkinje fibres
- Prolonged repolarization of mid-myocardial “M-cells”
- After-potentials resulting from mechanical forces in the ventricular wall

Features of Normal U Waves

- The U wave normally goes in the same direction as the T wave
- U -wave size is inversely proportional to heart rate: The U wave grows bigger as the heart rate slows down
- U waves generally become visible when the heart rate falls below 65 bpm
- The voltage of the U wave is normally $< 25\%$ of the T-wave voltage: disproportionately large U waves are abnormal
- Maximum normal amplitude of the U wave is 1-2 mm

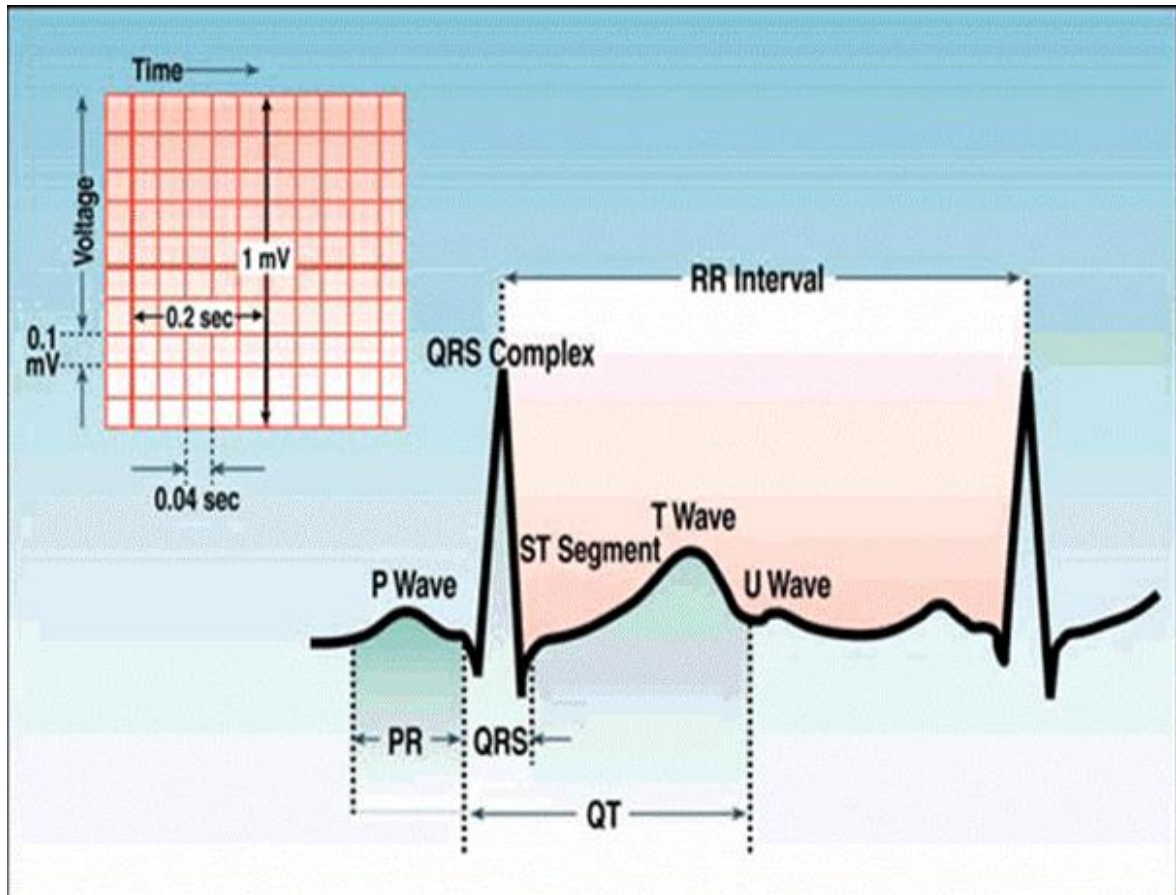


Figure 2. 6: U-waves in ECG signal [2.2].

2.2.5 ECG Register

An electrocardiogram (ECG or EKG) is a register of the heart's electrical activity. Just like skeletal muscles, heart muscles are electrically stimulated to contract. This stimulation is also called activation or excitation. Cardiac muscles are electrically charged at rest. The inside of the cell is negatively charged relative to the outside (resting potential). If the cardiac muscle cells are electrically stimulated, they depolarize (the resting potential changes from negative to positive) and contract. The electrical activity of a single cell can be registered as the action potential [2.2]. As the electrical impulse spreads through the heart, the electrical field changes continually in size and direction. The ECG is a graph of these electrical cardiac signals.

2.2.4 The Electric Discharge of the Heart

Sinoatrial node (SA node) contains the fastest physiological pacemaker cells of the heart; therefore, they determine the heart rate [2.4]. First the atria depolarize and contract. After that the ventricles depolarize and contract. The electrical signal between the atria and the

ventricles goes from the sinus node via the atria to the AV-node (atrioventricular transition) to the His bundle and subsequently to the right and left bundle branches, which end in a dense network of Purkinje fibers. The depolarization of the heart results in an electrical force which has a direction and magnitude; an electrical vector. This vector changes every millisecond of the depolarization. In the animation vectors for atrial depolarization, ventricular depolarization and ventricular repolarization are shown.

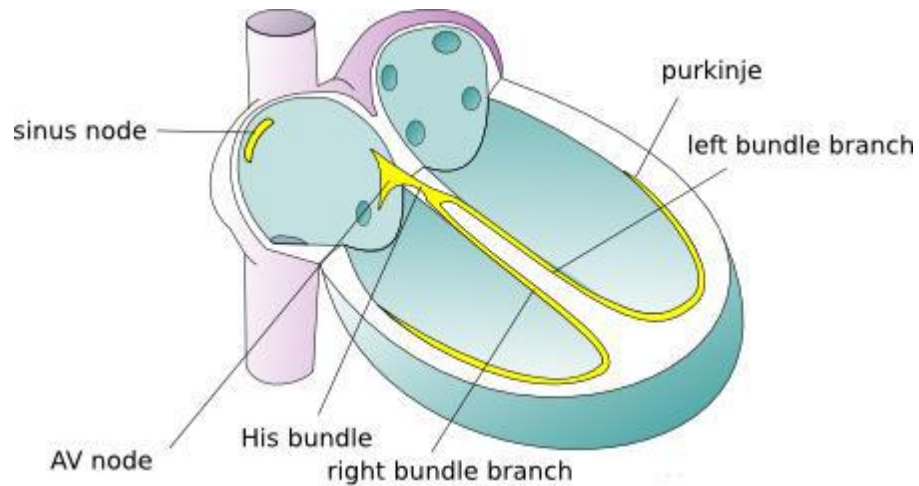


Figure 2. 7: The conduction system of the heart [2.2].

2.3 Overview of Basic Noises in ECG Signal

Electrocardiographic (ECG) signals may be corrupted by various kinds of noise. Typical examples are:

- power line interference
- electrode contact noise
- motion artifacts
- muscle contraction (Electromyogram, EMG)
- baseline drift and ECG amplitude modulation with respiration
- instrumentation noise generated by electronic devices used in signal processing, and
- Electrosurgical noise,

and other, less significant noise sources [2.5].

2.3.1 Power-line Interference Noise (PLI)

Power line interference (PLI) coupled to signal carrying cables is particularly troublesome in medical equipment. Cables carrying signals from the examination room to the monitoring equipment are prone to electromagnetic interference (EMI) of frequency (50 Hz or 60 Hz) by ubiquitous supply lines. Sometimes the recordings (like ECG or EEG) are totally dominated by this type of noise. Reducing (filtering) such PLI signal is a significant challenge given that the frequency of the power line signal lies within the frequency range of the ECG and EEG signals. [2.6,2.7] PLI is a significant source of noise during bio-potential measurements. EMI degrades the signal quality and disturbs the tiny features that may be crucial for monitoring and diagnosis, and it is observed that it can strongly distort bio potentials. Various biomedical signals contain distinct features in the time-domain analysis. It is seen that the PLI can contaminate the ECG recordings, due to differences in the electrode impedance and stray currents through the patient, cables, or in instruments with a floating input for a higher patient safety [2.8]. An ECG signal corrupted with PLI is illustrated in Figure 2.8.

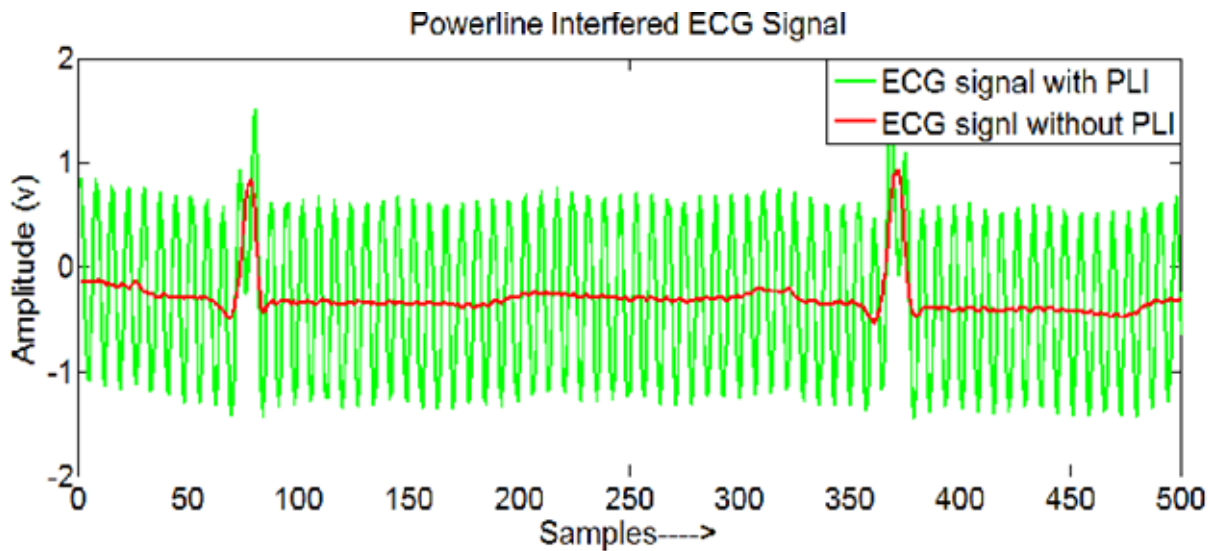


Figure 2. 8: ECG signal + power line Interference [2.6].

Capacitive and inductive coupling are the mechanisms that contribute to Power line interference. Capacitive coupling refers to the transfer of energy between circuits by means of a capacitance present between the circuits [2.9]. The coupling capacitance decreases with increase in the separation between the circuits. On the other hand, Inductive coupling is caused by inductance which exists between the conductors. Current flowing through the wire

tends to produce a magnetic flux that induces a current in adjacent circuits. The structure of the conductors as well as the separation between them decides the value of the mutual inductance, and thus the degree of the inductive coupling. Typically, high frequency noise is contributed by capacitive coupling and inductive coupling introduces low frequency noise. Inductive coupling is the significant mechanism of power line interference in electrocardiology.

2.3.2 Electrode Contact Noise

Electrode contact noise is caused by the loss of contact between the electrode and the skin, which effectively disconnects the measurement system from the subject. The noise is of duration 1s. [2.10]

Position of the heart with respect to the electrodes (variation) and changes in the propagation medium between the heart and the electrodes initiate Electrode contact noise. This causes sudden changes in the amplitude of the ECG signal, and low frequency baseline shifts. In addition, poor conductivity between the electrodes and the skin both reduces the signal amplitude of the ECG signal and thereby increases the probability of disturbances (by reducing SNR). The mechanism responsible for baseline disturbances is electrode-skin impedance variation. The larger the electrode-skin impedance, smaller are the relative impedance change which is required to cause a major shift in the baseline of the ECG signal. If the skin impedance is significantly high, it might be impossible to detect the signal features reliably in the presence of body movement [2.11]. Sudden changes in the skin-electrode impedance induce sharp baseline transients which decay exponentially to the baseline value. This transition may occur only once or rapidly several times in succession. Amplitude of the initial transition and the time constant of the decay are the major characteristics of such noise.

2.3.3 Motion Artifact

Motion artifacts are baseline changes which are caused by electrode motion. Usually vibrations, movement, or respiration of the subject contribute to motion artifacts. The peak amplitude and duration of the artifact depend on various unknown quantities such as the electrode properties, electrolyte properties, skin impedance, and the movement of the patient. In ECG signal, the baseline drift occurs at an unusually low frequency (approximately

0.014Hz), and most likely results from very slow changes in the skin-electrode impedance. This noise can also be observed on the Fourier power spectrum, the large peak nearest to DC [2.12].

2.3.4 Electromyography Noise (EMG)

Contraction of the muscles besides the heart contributes to the EMG noise. When other muscles in the vicinity of the electrodes contract, generation of depolarization and repolarization waves takes place and these waves are picked up by the ECG. The gravity of the crosstalk depends on the amount of muscular contraction (subject movement), and the quality of the probes. It is well established fact that the amplitude of the EMG signal is stochastic (random) in nature and is typically modeled by a Gaussian distribution function [2.12]. The mean of the noise can be assumed to be zero however the variance is dependent on the environmental variables and will change depending on the conditions. While the actual statistical model is unknown, it should be noted that the electrical activity of muscles during periods of contraction can generate surface potentials comparable to those from the heart, and could completely drown out the desired signal. EMG noise is common in subjects with uncontrollable tremor, disabled persons, kids and persons fearing the ECG procedure.

2.3.5 Baseline Wander

Baseline wander is a low-frequency noise component present in the ECG signal. This is mainly due to respiration, and body movement. Baseline wander have frequency greater than 1Hz. This low frequency noise, Baseline wander causes problem in detection and analysis of peak.

2.3.6 Burst Noises

Burst noise is typically classified as a white Gaussian noise (WGN) which appear on a subset of leads for a very short duration, examples of these noises are electrode pop noise, electrode motion artifact, electro surgical noise, instrumentation noise etc. [2.13]. The frequency ranges for these noises are not well defined.

2.3.7 Instrumentation Noise

The electrical equipment which is used in ECG measurements also contributes noise. Electrode probes, cables, signal processor/amplifier, and the Analog-to-Digital converter are the major sources of this form of noise. Unfortunately, instrumentation noise cannot be eliminated, but it can be reduced through higher quality equipment and careful circuit design. One type of electrical noise is resistor thermal noise (also known as Johnson noise). Random fluctuations of the electrons due to thermal agitation produce this noise. The power spectrum is given as

$$\bar{v}^2 = 4KTR$$

Where k is the Boltzmann's constant, T is the temperature, and R is the resistance. This equation suggests that the resistor thermal noise is white for all frequencies; however, at frequencies larger than 100 Hz the power spectrum starts to drop off. Another form of noise, called flicker noise, is important in ECG measurements, due its low frequency. The actual mechanism that causes this type of noise is not yet understood, but one widely accepted theory is that it is caused by the energy traps which occur between the interfaces of two materials. It is believed that the charge carriers get randomly trapped/released and cause flicker noise. Flicker noise contributions would be most noticeable at the electrodes since the amplitude of the detected signal is on the order of millivolts [2.1].

2.4 Filtering

Almost all type of signal distortion or corruption can be modelled as an addition of frequency components. Even the rectification/clipping can be thought of as addition of harmonics. So, we have to work in the frequency domain. Time domain analysis will not help. Whenever we are in the frequency domain, to remove any component, filters are the things to use.

The frequency domain refers to the analysis of mathematical functions or signals with respect to frequency, rather than time. A time-domain graph shows how a signal changes over time, whereas a frequency-domain graph shows how much of the signal lies within each given frequency band over a range of frequencies. A frequency-domain representation can also include information on the phase shift that must be applied to each sinusoid in order to be able to recombine the frequency components to recover the original time signal [2.14].

In signal processing, a filter is a device or process that removes some unwanted components or features from a signal. Filtering is a class of signal processing, the defining feature of

filters being the complete or partial suppression of some aspect of the signals. Most often, this means removing some frequencies or frequency bands. However, filters do not exclusively act in the frequency domain; especially in the field of image processing many other targets for filtering exist. Correlations can be removed for certain frequency components and not for others without having to act in the frequency domain [2.15].

The transfer function of a filter is most often defined in the domain of the complex frequencies. The transfer function $H(z)$ of a filter is the ratio of the output signal $Y(z)$ to that of the input signal $X(z)$ as a function of the complex frequency s :

$$H(z) = \frac{Y(z)}{X(z)} \quad (2.1)$$

where $s = \sigma + j\omega$

Some terms used to describe linear filters-

- ✓ Cutoff frequency is the frequency beyond which the filter will not pass signals. It is usually measured at a specific attenuation such as 3 dB.
- ✓ Roll-off is the rate at which attenuation increases beyond the cut-off frequency.
- ✓ Transition band, the (usually narrow) band of frequencies between a passband and stopband.
- ✓ Ripple is the variation of the filter's insertion loss in the passband.
- ✓ The order of a filter is the degree of the approximating polynomial and in passive filters corresponds to the number of elements required to build it. Increasing order increases roll-off and brings the filter closer to the ideal response [2.15].

2.5 Multirate System

Linear time-invariant systems operate at a single sampling rate i.e. the sampling rate is the same at the input and at the output of the system, and at all the nodes inside the system. Thus, in an LTI system, the sampling rate doesn't change in different stages of the system. Systems that use different sampling rates at different stages are called the multirate systems. The multirate techniques are used to convert the given sampling rate to the desired sampling rate, and to provide different sampling rates through the system without destroying the signal components of interest [2.16].

2.6 Multistage Systems

When the decimation factor M can be factored into the product of integers, $M = M_1 \times M_2 \times \dots \times M_K$, instead of using a single filter and factor-of- M down-sampler the overall decimator can be implemented as a cascade of K decimators. Such a cascade implementation, called a multistage decimator, is shown in Figure 2.9. In the same manner, the factor-of- L interpolator expressible by $L = L_1 \times L_2 \times \dots \times L_K$, can be implemented as a cascade of K interpolators as depicted in Figure 2.10. The cascade implementation scheme of Figure 2.10 is called the multistage interpolator.

The multistage structure from Figure 2.9 replaces the single stage decimator of the factor $M = M_1 \times M_2 \times \dots \times M_K$. The transfer function $H(z)$ of the equivalent single-stage decimation filter can be obtained by applying the third identity to the implementation scheme of Figure 2.9. The cascade of K decimators of Figure 2.9 gives the following equivalent transfer function $H(z)$,

$$H(z) = H_1(z)H_2(z^{M_1})H_3(z^{M_1M_2}) \dots H_K(z^{M_1M_2 \dots M_{K-1}}) \quad (2.2)$$

Thereby, the single-stage structure indicated in Figure 2.11 is equivalent to the structure of Figure 2.9.

Similarly, the overall transfer function for the K stage interpolator is obtained when applying the sixth identity to the multistage implementation structure of Figure 2.10. This way, we obtain,

$$H(z) = H_1(z)H_2(z^{L_1})H_3(z^{L_1L_2}) \dots H_K(z^{L_1L_2 \dots L_{K-1}}) \quad (2.3)$$

The corresponding single-stage equivalence for the K stage interpolator is indicated in Figure 2.12.



Figure 2. 9: Multistage implementation of decimator.

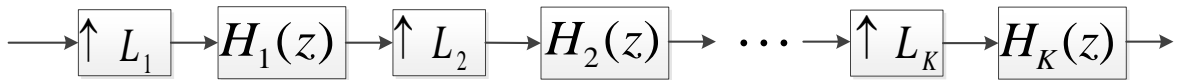


Figure 2. 10: Multistage implementation of interpolator.

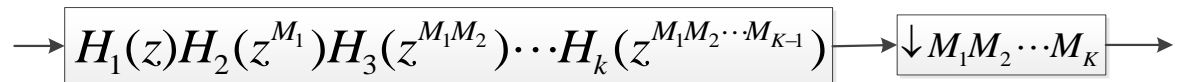


Figure 2. 11: The single-stage equivalence for the multistage structure of Figure 2.9.

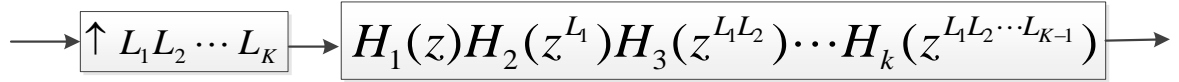


Figure 2. 12: The single stage equivalence for the multistage structure of Figure 2.11.

The multistage structures are very useful for implementing large sampling-rate conversion factors. A single decimation/interpolation filter with a very narrow passband, usually inconvenient for the design and implementation, is replaced with the cascade of simpler filters. The specifications for those individual filters are significantly relaxed since the overall filter specification is shared between several lower-order filters.

2.7 Atrial Fibrillation

Cardiac arrhythmias are caused by abnormal electrical activity of the heart. Among them, Atrial Fibrillation (AF) is one of the most common types [2.17]. It has a prevalence of about 1–2 % in the general population. More than 6 million Europeans and about 2 million US-Americans suffer from AF. Among the elderly, the incidence of AF significantly increases up to 5–15 % at the age of 80 years above [2.17]. AF is characterized by uncoordinated atrial activation due to disrupted electrical pathways and structural changes in the heart [2.18]. In AF, the electrical impulse originates from different areas in the atria. This causes the atria to quiver rather than to contract, which results in insufficient heart function. The exact mechanism which causes AF remains uncertain. The different theories involve two main processes: rapidly depolarizing foci, and reentry circuits. The rapidly depolarizing foci are usually located in the superior pulmonary veins, but can also occur in the right atria, or (more rarely) in superior vena cava or coronary sinus. The electrical impulses do not follow the normal conduction path, but instead they form electrical reentry loops in the atria. During AF, the refractory period of the conduction cells is usually shortened, and activation of the atrial conduction cells often occurs immediately after the refractory period [2.19].

2.8 The Heart in Normal

The heart consists of a left and a right part, each incorporating two chambers; the atrium and the ventricle. The two sides are divided by a muscular wall, called the septum. Four different valves control the direction of the blood flow; the atrio ventricular valves between the atria and the ventricles, and the pulmonary and aortic valves between the ventricles and the arteries. The wall of the heart, called myocardium, is mainly composed of muscle cells which

exercise mechanical force during contraction. The mechanical force of the muscle cells is triggered by electrical impulses throughout the heart. Fig. 2.13 shows the anatomy of the heart. During one cardiac cycle a sequence of mechanical events occur, starting when blood in the right atrium is forced into the right ventricle by contraction of the atria. The blood in the right atria has been collected from all veins in the body, except for the veins from the lungs. When the right ventricle is filled with blood, it contracts and forces the blood into the pulmonary artery, to the lungs where it is oxygenated. The oxygenated blood passes through the pulmonary veins to the left atrium, which, once it is filled, contracts and forces the blood to the left ventricle. When the left ventricle contracts, the blood flows to all arterial vessels in the body, except for the lungs, into the venous system and back to the right atrium again. The cardiac cycle consists of two phases; activation (contraction) and recovery (relaxation) which in electrical terms are referred to as depolarization and repolarization, respectively. Depolarization is a rapid change of the membrane potential of a cell, spreading to neighboring cells so that the electrical impulse propagates. After depolarization, the cell immediately starts its repolarization to return to its resting state.

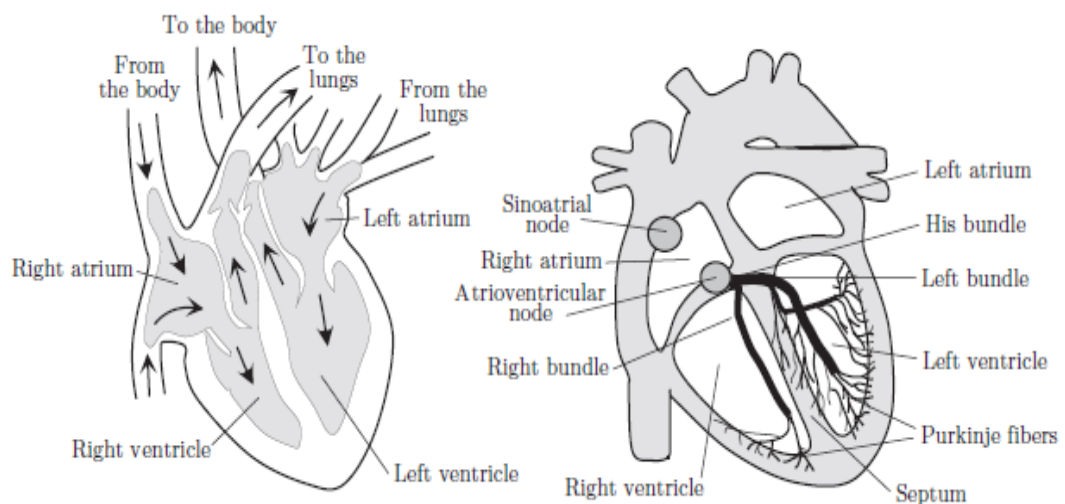


Figure 2. 13: Anatomy of the heart [2.20].

During this period of time, called refractory period, the cell cannot depolarize. In the normal heart, the cardiac cycle is initiated by an electrical impulse originating from the sinoatrial (SA) node, the natural pacemaker of the heart situated in the right atrium. The electrical impulse propagates through the right and left atria to the atrio ventricular (AV) node, where it is collected and delayed before it continues to the bundle of His, being the only electrical connection between the AV node and the ventricles. The ventricular conduction system

consists of the rapidly conducting left and right bundle branches and the Purkinje network. The rate of electrical impulses which causes the heart to beat is determined by the autonomic nervous system.

2.9 The Heart During AF

In AF, the electrical impulse originates from different areas in the atria. This causes the atria to quiver rather than to contract, which results in insufficient heart function. The exact mechanisms of AF remain uncertain. The different theories involve two main processes: rapidly depolarizing foci, and reentry circuits. The rapidly depolarizing foci are usually located in the superior pulmonary veins, but can also occur in the right atria, or (more rarely) in superior vena cava or coronary sinus. The electrical impulses do not follow the normal conduction path, but instead they form electrical reentry loops in the atria. During AF, the refractory period of the conduction cells is usually shortened, and activation of the atrial conduction cells often occur immediately after the refractory period [2.21]. Of all electrical impulses coming from the atria during AF, only a limited number of signals actually reach the ventricles, since the AV node prevents the heart from racing. Still, the heart rate during AF is abnormally high. While AF is not generally considered life-threatening, there is a possibility of blood clots forming in the atria which leads to increased risk of stroke. One of every 6 strokes occur in patients with AF [2.22].

2.10 Diagnosis and Treatment - Challenges in AF

Proper diagnosis is essential for proper treatment. There are various methods to detect AF, such as, Electrocardiography (ECG), Echocardiography, Transesophageal Echocardiography, Chest X-Ray. However, AF is usually diagnosed from the surface ECG to confirm its presence.

Today, there is no clinical test available that can predict the natural history of AF and the outcome of treatment. Since an ECG is recorded from practically all AF patients, it is desirable to classify AF from the ECG signal, to help physicians in deciding which treatment is appropriate for a specific patient. The characteristics of the ECG signal during AF varies not only between different patients, but also in the same patient over time. One important challenge is to track such changes in long term ECG recordings which usually are recorded during ambulatory conditions.

2.11 ECG Signal for AF Detection

The ECG signal is a representation of the bio-potentials that is generated by the muscles of the heart. During Normal Sinus Rhythm (NSR), each heartbeat in the ECG signal consists of a P wave, a QRS complex and a T wave. The P wave corresponds to atrial activation, the QRS complex to activation of the ventricles, and the T wave to ventricular recovery, as seen in Fig. 2.14. An example of ECG signal, recorded during NSR, is given in Fig. 2.15(a). In AF, the P wave is replaced by an undulating baseline, where the waves are referred to as f waves, as shown in Fig. 2.15(b).

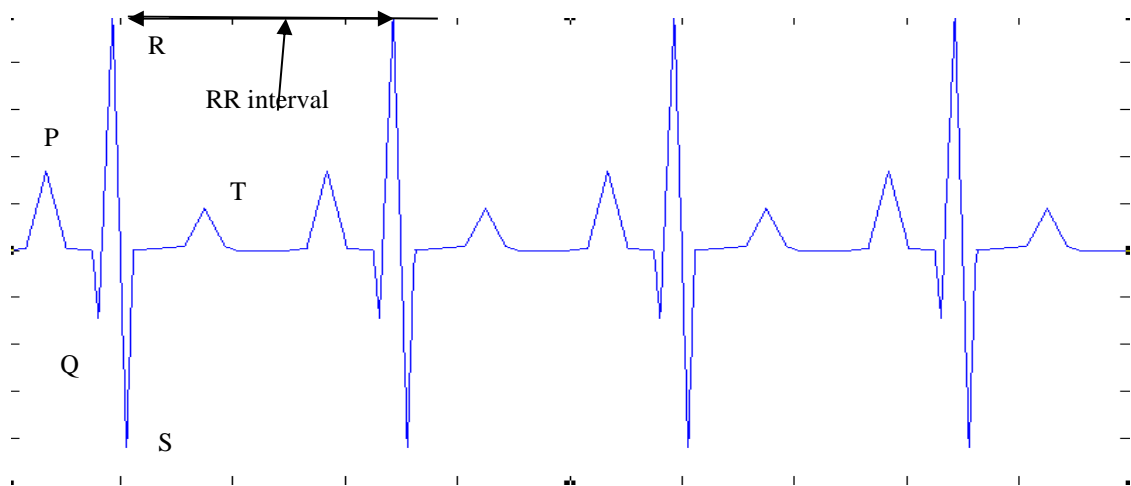


Figure 2. 14: Different parts of the ECG signal during NSR [2.16].

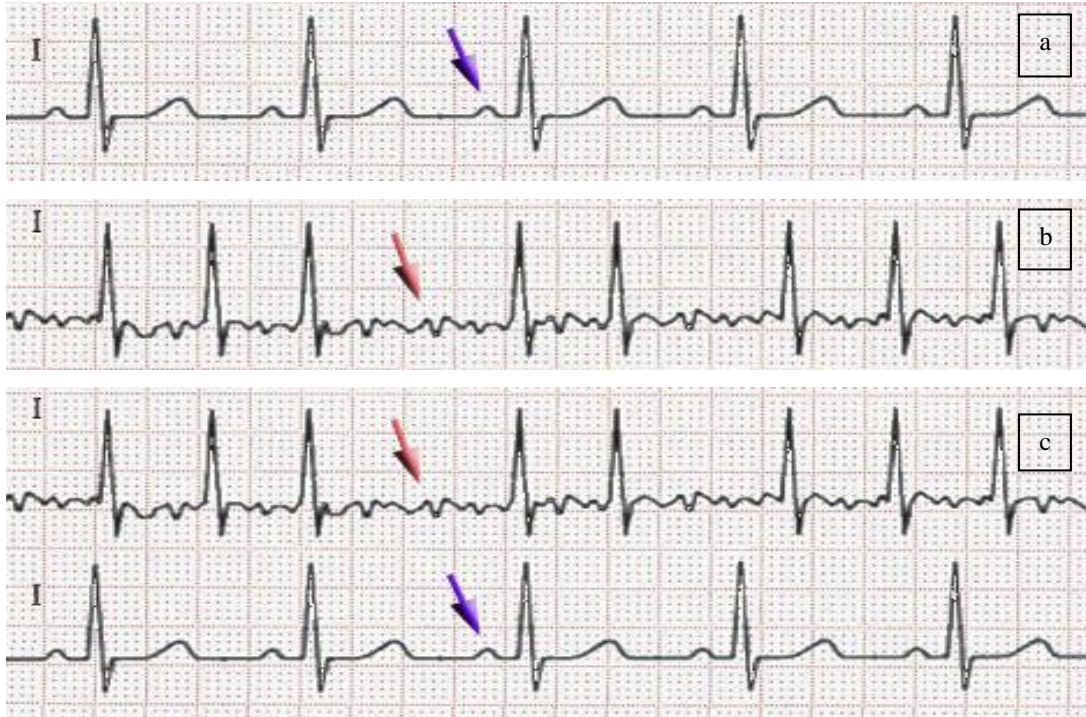


Figure 2. 15: Examples of ECG signals during (a) NSR and (b) AF and (c) both NSR and AF [2.23].

During AF, electrical discharges conducted from the atrium into the ventricles are irregular and as a result, the heart rate becomes irregular and, usually rapid and also the electrical Atrial Activity (AA) is disorganized [2.24]. Both of these characteristics can be easily detected by the analysis of an ECG signal by noticing the irregularity of R-R intervals and the absence of the P-wave [2.24]. So, there are basically two methods for the detection of AF from the ECG signal. They are the RR Irregularity and the AA. Any one of the two methods can be followed to detect the AF. The combination of the RR Irregularity and the AA can also be used to get enhanced detection performance. The RR irregularity is the most common method and very frequently used. This method is much easier because the R wave is the most prominent characteristics in the ECG signal, so it is relatively easy to detect. In this thesis, only the RR Irregularity is used to detect the AF from an ECG signal.

2.12 History of AF Detection

Issues relating to clinical significance of rhythm classification and the impetus for improving the accuracy of atrial tachyarrhythmia estimation have motivated the development of innovative computerized AF detectors. Since the early 1980s, a series of sophisticated methods have been investigated to cope with the challenges of AF detection [2.25].

Methods for the detection of AF vary in terms of type, time, cost, and accuracy. Recently, methods for AF detection focus on statistical analysis, with the goal of earlier detection in real-time. Methods for detecting AF found in literature are identified as [2.26],

- Diagnostic Testing
- Biological Imaging
- Statistical Analysis
- Electrocardiography
- Echocardiography
- Transesophageal Echocardiography
- Chest X-ray

2.12.1 Diagnostic Testing

Diagnostic testing is one method of detection and is usually the result of symptomatic patients. Some of these tests include long-term Holter-monitoring, ECG interpretation and blood tests. Currently, the most common method for detection is through continuous Holter-monitoring [2.27]. The Holter monitor is attached to the patient with 3 or 5 leads that traces the heart's signals over a period of 24-48 hours. Then, a certified technician or doctor is required to look through the entire tracing to diagnose AF. There are some problems with this; first, there's a lot of noise generated when using Holter monitors. Paroxysmal AF appears for very brief segments and may be masked by noise, leaving those short segments undetectable. The ECG tracings also require very thorough analysis. It is apparent that looking at 24 or even 48 hours' worth can be extremely time-consuming, and irregularities can be easily overlooked.

2.12.2 Biological Imaging

Biological imaging is a method that involves the analysis of images obtained from echocardiograms and chest X-rays. Echocardiography uses sound waves to create an image of a patient's heart [2.27]. It provides information about the size and shape of the heart and can provide information on any structural changes that may have occurred in the heart, which is a characteristic of AF. This type of imaging is not helpful in early detection, as these structural changes are usually observed in chronic, permanent cases of AF.

2.12.3 Statistical Analysis

Current methods for detection of AF focus on using mathematical models and statistical methods for early AF detection. Those methods utilize statistics for detection and diagnosis, yet each provides restrictions and limitations that must be addressed.

2.12.4 Electrocardiography

Electrocardiography or ECG is the most commonly used for AF detection for its high accuracy and simplicity.

2.12.5 Echocardiography

Echocardiography test shows the size and shape of the heart as well as how well the chambers and valves are operating. During the test a transducer is moved around the chest which emits sound waves through the chest and heart. The sound waves bounce off of the shape of the heart and a computer converts the information into an image on a monitor.

2.12.6 Transesophageal Echocardiography

Transesophageal echo also emits sound waves into the heart that produce an image on a monitor. During this procedure, however, the transducer is attached to a long tube which is inserted into the patient's esophagus.

2.12.7 Chest X-ray

A chest x-ray uses electromagnetic waves to create an image of the heart and lungs using ionizing radiation. Since the different tissues inside your body absorb the radiation differently an image is produced that can show an increase in fluid in the lungs as well as other issues caused by AF.

However, most of the literature describe that AF detection is done based upon two main character traits of this type of arrhythmia shown in a surface ECG: (i) RR interval irregularity (i.e., chaotic behavior of HRV), and (ii) P-wave absence (PWA) or F-wave substitution (i.e., very low amplitude waveforms of odd morphologies) resulting from the abnormal rapid atrial AA. Although P waves or cardiac AA can be an alternative clue in the detection of AF,

the absence or presence of P waves are not readily identifiable as various types of high-intensity noise often coexist in ECGs, which may lead to a low degree of predictive accuracy. In addition, the relationship between AA in the surface ECG and the diverse mechanisms of AF has not yet been well delineated [2.28]. Due to the challenges in detecting AA in ECG measurements, detection techniques based on inferences from RR intervals are preferred to produce relatively robust outcomes [2.29-2.30, 2.26].

2.13 Review of Related Research Work on Thesis

Wavelet transforms have been used in the field of signal and image processing. Recently research worked on wavelet construction called lifting scheme, has been established by Wim Sweldens and Ingrid Daubechies [2.31]. This is also referred to wavelet 9/7 filter. This scheme was developed on FIR-based discrete transform. They considered, the input signal is fed into a low pass filter and high pass filter separately. The outputs of the two filters are then subsampled. The original signal can be reconstructed by synthesis filters h and g which take the up-sampled Lowpass and high pass as inputs. This scheme is also used Laurent polynomial representation of filter and Euclidean algorithm. These scheme shows some limitations on sampling methods.

Frequency converters sampling methods and narrow band filtering are known, allowing significant computational efficiency [2.32, 2.33]. However, current design procedures for these multistage and multilayer filters address the specification of each phase individually, rather than simultaneously optimizing all of the filter phases [2.34]. The authors [2.35] formulate an algorithm that optimizes multi-stage adaptive coefficients and also provides sufficient conditions for multi-track filter identification. A multilayer digital filter (MDF) is a digital filter that changes the input sampling frequency from the input signal to another signal. There are many applications in communication, image processing, digital audio and multimedia. In [2.36], the modern DSP system uses MDF with three factors. First of all, MDF is used in two digital systems with a different sampling rate. Second, MDF is the best approach to solving the complex filtering problem. Third, multilayer filtering is used in the construction of the multilayer filter bank.

Most of the algorithms/methods existing in literature to detect AF from ECG signal are based on the analysis of both RRI and AA.

2.13.1 RR Irregularity (RRI)

The R wave is the most prominent characteristic within the ECG, making it relatively simple to detect. Therefore, algorithms that detect AF based on RRI are the most common in the literature. Five algorithms based on RRI are selected to realize: Moody et al. [2.25], based on Markov Models (MM); Logan et al. [2.37] using a simple variance parameter; Linker et al. [2.38], that used a statistical framework combination; Tatento et al. [2.39], which applied Kolmogorov Smirnov test; and Cerutti et al. [2.40], which used an autoregressive modeling and compares RRI with white noise.

2.13.2 Atrial Activity (AA)

P wave is absent in the AA within AF ECGs and replaced by a fibrillatory wave. AA can be analyzed in both time and frequency domains. Time domain consists of detecting the P wave or finding the P wave absence (PWA). Frequency spectrum analysis (FSA) requires cancellation of ventricular activity (QRS complex and T wave) and Fourier analysis of the remaining AA. Electrical AA on AF ECG is characterized by higher energy concentration in the band of 4-10 Hz as compared to normal ECGs. One algorithm is selected based on AA for illustration. Slocum et al.'s algorithm [2.41] was based on the AA analysis to identify AF. Firstly, QRS-T cancellation was done and the remaining atrial signal is studied. In case P wave was detected, the signals were classified as non-AF. Otherwise, FSA was calculated and it was considered as AF if the total spectral power in the band of 4-9 Hz was more than 32% of the total spectrum.

2.13.3 Combination of RRI and AA

Combination of both RRI and AA (PWA and/or FSA) are used to enhance detection performance. Three algorithms are selected in this category for realization. Schmidt et al. [2.42] combined RRI using MM, with PWA and FSA. Babaezaideh et al. [2.43] added to RRI PWA based on the position and morphology of the P wave. Finally, Couceiro et al. [2.44] combined the three main physiological characteristics of AF (RRI, PWA and FSA) and classified using Neural Networks (NNs) model created previously.

Those algorithms reported in the literature exhibits the sensitivity (Se), specificity (Sp), positive predictive value (PPV) and error, ranging from 62.80~97.64%, 77.46~96.08%, 64.90~92.75% and 5.32~28.39%, respectively.

2.14 Summary

In this chapter, basic topics of ECG is discussed which is very important in analysis of ECG signal. It also discusses how ECG signal is generated and how to acquire it using electrodes. Various ECG waves are also discussed. Various noises in ECG signal such as power line interference, EMG noise, baseline shift, abrupt shift in base line, electrosurgical noise etc. are also mentioned in this chapter. This chapter outlines the literature related to the ECG signal denoising and AF detection. From these literatures, there are some lack of novelty work. We have tried to find the problem statement of ECG diagnosis and QRS detection.

REFERENCES

- [2.1] J. R. Mou, "Thesis: De-noising of ECG signal using FIR filter and QRS detection", *Khulna University of Engineering & Technology (KUET)*, May 2017.
- [2.2] <http://www.heart.org/HEARTORG/Conditions/HeartAttack/Symptoms>
- [2.3] <http://www.nhs.uk/Conditions/electrocardiogram/Pages/Introduction.aspx>
- [2.4] P. Kligfield, L.S. Gettes, J. J. Bailey, R. Childers, B. J. Deal, E. W. Hancock, G. V. Herpen, J. A. Kors, P Macfarlane, D. M. Mirvis, O. Pahlm, P. Rautaharju, and G. S. Wagner, "Recommendations for the standardization and interpretation of the electrocardiogram: part I", *International Society for Computerized Electrocardiology*, 115(10) pp. 1306-24, March 2007.
- [2.5] G. M. Friesen, T. C. Jannett, M. A. Jadallah, S. L. Yates, S. R. Quint, and H. T. Nagle, "A Comparison of the Noise Sensitivity of Nine QRS Detection Algorithms", *IEEE Transactions on Biomedical Engineering*, Vol 37, No. 1, pp. 85 -98, 1990.
- [2.6] L. Sörnmo, P. Laguna, "Bioelectrical signal processing in cardiac an neurological applications", *Elsevier Academic Press*; 2005.
- [2.7] R. M. Rangayyan, "Biomedical signal analysis: a case-study approach", *IEEE Press Seminar on Biomedica. Engineering*, 2002.
- [2.8] C. Levkov, G. Mihov, R. Ivanov, I. Daskalov, I.I. Christov, I. Dotsinsky, "Removal of power-line interference from the ECG: a review of the subtraction procedure", *Biomed. Eng. Online* 4 (50) 2005.
- [2.9] H. Wan, R. Fu and L. Shi, "The Elimination of 50 Hz Power Line Interference from ECG Using a Variable Step Adaptive Algorithm", *Life Science Journal*, 3(4), 2006.
- [2.10] M. Gary, F. Thomas, C. Jannett, M. A. Jadallah, S. L. Yates, S. R. Quint and H. T. N Nagle, "A Comparison of the Noise Sensitivity of Nine QRS Detection Algorithms", *IEEE Transactions on Biomedical Engineering*, Vol,37, No. 1, March 1990.
- [2.11] S. A. Israel, J. M. Irvine, A. Cheng, M. D. Wiederhold, and B. K. Wiederhold, "ECG to Identify Individuals", *Pattern Recognition, Elsevier*, Vol. 38(1), pp.133-142, January 2005.
- [2.12] P. Tikkanen, "Characterization and Application of Analysis Methods for ECG and Time Interval Variability Data", *Ph.D. dissertation*, University of Oulu, Oulu, Finland, 1999.

- [2.13] F.Castells, P. Laguna, L. S’ornmo, A. Bollmann and J. Roig, “Principal component analysis in ECG signal processing”, *EURASIP J. Adv. Signal Process*, 2007.
- [2.14] S. A. Broughton and K. Bryan, “Discrete Fourier Analysis and Wavelets: Applications to Signal and Image Processing”, *John Wiley & Sons, Inc.* 22 February 2011.
- [2.15] S. K. Mitra, “Digital Signal Processing: A Computer-Based Approach,” 4th Edition, *The McGraw-Hill Companied, Inc.* 2011.
- [2.16] L. Milić, “Multirate Filtering for Digital Signal Processing: MATLAB Applications”, *Ljiljana Milić Pub.* Chapter 2-4, pp 23-111.
- [2.17] C. Brüser, J. Diesel, M.D.H. Zink, S. Winter, P. Schauerte and S. Leonhardt, “Automatic Detection of Atrial Fibrillation in Cardiac Vibration Signals”, *IEEE J. Biomed. Health Informatics*, vol. 17, no. 1, pp. 162-171, 2013.
- [2.18] C. A. Sanoski and D. Pharm, “Clinical, Economic, and Quality of Life Impact of Atrial Fibrillation”, *J. Manag. Care Pharm.* 15(6 Suppl B): S4-9, August 2009.
- [2.19] S. Al-Khatib, W. Wilkinson, L. Sanders, E. McCarthy and E. Pritchett, “Observations on the Transition from Intermittent to Permanent Atrial Fibrillation”, *Am. Heart J.*, vol. 140, pp. 142– 145, 2000.
- [2.20] V. Fuster, “ACC/AHA/ESC Guidelines for the Management of Patients with Atrial Fibrillation”, *Circulation*, vol. 104, pp. 2118–2150, 2001.
- [2.21] A. Bollmann, N. Kanuru, K. McTeague, P. Walter, D. B. DeLurgio, and J. L. Langberg, “Frequency Analysis of Human Atrial Fibrillation Surface Electrocardiogram and its Response Ttoibutilide”, *Am. J. Cardiol.*, vol. 81, pp. 1439–1445, 1998.
- [2.22] J. Slocum, E. Byrom, L. McCarthy, A. Sahakian and S. Swiryn, “Computer Detection of Atrioventricular Dissociation from Surface Electrocardiograms during Wide QRS Complex Tachycardia”, *Circulation.*, vol. 72, pp. 1028–1036, 1985.
- [2.23] The Wikipedia website. [Online]. Available: http://en.wikipedia.org/wiki/Atrial_fibrillation
- [2.24] N. Larburu, T. Lopetegi and I. Romero, “Comparative study of algorithms for Atrial Fibrillation detection”, *2011 Computing in Cardiology*, Hangzhou, pp. 265-268. 2011.

- [2.25] G. Moody and R. Mark, “A New Method for Detecting Atrial Fibrillation Using RR Intervals, Computers in Cardiology”, Aachen: *IEEE Computer Society Press*, vol. 10, pp. 227–230, 1983.
- [2.26] J. Lee, B. Reyes, D. McManus, O. Mathias and K. Chon, “Atrial Fibrillation Detection Using an Iphone 4S”, *IEEE Trans Biomed. Eng.*, vol. 60, pp. 203–206, 2013.
- [2.27] National Institutes of Health, Atrial Fibrillation, Online Available: <http://www.nhlbi.nih.gov/health/dci/Diseases/af/af_diagnosis.html>, 5th May 2014.
- [2.28] S. Petrutiu, J. Ng, G. Nijm, H. Al-Angari, S. Swiryn and A. Sahakian, “Atrial Fibrillation and Waveform Characterization”, *IEEE Eng. Med. Bio. Mag.*, vol. 25, no. 6, pp. 24–30, 2006.
- [2.29] J. Lian, L. Wang and D. Muessig, “A Simple method to Detect Atrial Fibrillation Using RR Interval”, *Am J Cardiol*, vol. 107, no.10, pp. 1494–1497.
- [2.30] C. Huang, S. Ye, H. Chen, D. Li, F. He and Y.Tu, “A Novel Method for Detection of the Transition Between Atrial Fibrillation and Sinus Rhythm”, *IEEE Trans Biomed Eng*, vol. 58, no. 4, pp. 1113–1119, 2011.
- [2.31] I. Daubechies and W. Sweldens, “Factoring Wavelet Transforms into Lifting Steps”, *J. Fourier Anal. Appl.*, vol. 4, no. 3, pp. 247 – 269, May 1998.
- [2.32] R. E. Crochiere and L. R. Rabiner, “Multirate Digital Signal Processing”, Publisher: *Pearson; 1st edition*, ISBN-13: 978-0136051626, March 21, 1983.
- [2.33] P. P. Vaidyanathan, “Multirate System and Filter Banks”, *Publisher: Prentice Hall; 1 edition*, ISBN-13: 978-0136057185, October 1, 1992.
- [2.34] R.G. Shenoy, D. Burnside and T.W. Parks, “Linear Periodic Systems and Multirate Filter Design”, *IEEE Transactions on Signal Processing*, vol. 42, Issue: 9, pp.2242 – 2256, September 1994.
- [2.35] G. A. Williamson, S. Dasgupta and F. Minyue, “Multistage Multirate Adaptive Filters”, *IEEE International Conference on Acoustic, Speech, and Signal Processing conference Proceedings*, vol. 3, pp. 1534–1537, 1999.
- [2.36] E. Ifeachor and B. WQ. Jervis, “Digital Signal Processing: A Practical Approach, 2/E” Publisher,” *Pearson Education India*, ISBN 813708241, 9788131708248,2002.

- [2.37] B. Logan and J. Healey, “Robust Detection of Atrial Fibrillation for a Long-Term Tele monitoring System”, *Computers in Cardiology*, vol. 32, pp. 619-622, 2005.
- [2.38] D. Linker, “Long-Term Monitoring for Detection of Atrial Fibrillation, *Patent Application Publication*”, Seattle, US, 2006.
- [2.39] K. Tateno and L. Glass, “Automatic Detection of Atrial Fibrillation Using the Coefficient of Variation and Density Histograms of RR and RR Intervals”, *Medical & Biological Engineering & Computing*, vol. 39, no. 6, pp. 664–671, 2001.
- [2.40] S. Cerutti, L. Mainardi, A. Porta and A. Bianchi, “Analysis of the Dynamics of RR Interval Series for the Detection of Atrial Fibrillation Episodes”, *Computers in Cardiology*, vol. 24, pp. 77-80, 1997.
- [2.41] J. Slocum, A. Sahakian and S. Swiryn, “Diagnosis of Atrial Fibrillation from Surface Electrocardiograms Based on Computer-detected Atrial Activity”, *Journal of Electrocardiology*, vol. 25, pp. 1–8, 1992.
- [2.42] R. Schmidt, M. Harris, D. Novac and M. Perkhun, “Atrial Fibrillation Detection”, [WO Patent 2,008,007,236. Jan 18, 2008], *Patent Cooperation Treaty*, Eindhoven, Netherlands, 2008.
- [2.43] S. Babaeizadeh, R. Gregg, E. Helfenbein, J. Lindauer and S. Zhou, “Improvements in Atrial Fibrillation Detection for Real-Time Monitoring”, *Journal of Electrocardiology*, vol. 42, no. 6, pp. 522–526, 2009.
- [2.44] R. Couceiro, P. Carvalho, J. Henriques, M. Antunes, M. Harris and J. Habetha, “Detection of Atrial Fibrillation Using Model-Based ECG Analysis”, *19th International Conference on Pattern Recognition, Tampa, FL, IEEE*, pp. 1–5, 2008.

CHAPTER III

Multistage Multirate system

Chapter Outlines

- Introduction
- Materials and Methods
- Result and Discussion
- Summary
- References

CHAPTER III

Multistage Multirate system

3.1 Introduction

Manually, constructing a multi-stage poly-phase filter (i.e., decimation (reduced sampling rate), filtered and polyphase interpolation (increased sampling frequency) is a time-consuming and high-risk process. which we focus on in this thesis is the third factor. We developed the multistage multirate system support with multirate polyphase filters. This elimination process is easy for specific and computing a multistage multirate design. The main concept of proposed system, the input signal is decimated/interpolated and decomposed with M^{th} polyphase filter branch with sampling rate conversion is called analysis filter in the first stage. In the second stage, the input signal is decomposed with decimator then the polyphase multistage filter with converting the sampling rate to the rational factor L/M that represents the test filter of the system proposed. This process is continued for another stage for getting more and more smooth signal.

3.2 Materials and Methods

3.2.1 Database

In this thesis need to import ECG data for analysis and used the MIT-BIH Atrial Fibrillation database. This database includes 25 long term ECG recordings, as shown in Table 3.1. There are 23 of the records include two ECG recordings. Each individual recording are 10 hours in duration. Every recording has two signals and each of them sampled at 250 samples per second, 12-bit resolution over a range of 10 mV. Those ECG signals were recorded with a typical recording bandwidth of approximately 0.1 Hz to 40 Hz. The rhythm annotation files were prepared manually. These contain rhythm annotation of types AFIB (Atrial Fibrillation), AFL (Atrial Flutter), J (AV Junctional rhythm) and N (Used to indicate all other rhythm) [3.1]. Out of 25 long-term signals, 15 signals are selected for our analysis. This database also includes different types of noise such as powerline noise, baseline noise, EMG noise, abrupt shift noise and electrosurgical noise.

Table3. 1: List of original ECG signals taken from MIT-BIH Atrial Fibrillation Database [3.1].

Sl. No.	Original ECG signal (File #)	Selection Status	Additional Information
1	00735	Not selected	Signals unavailable
2	03665	Not selected	Signals unavailable
3	04015	Selected	
4	04043	Not selected	Block 39 is unreadable
5	04048	Selected	
6	04126	Selected	
7	04746	Selected	
8	04908	Selected	
9	04936	Not selected	Error in annotation
10	05091	Not selected	Error in annotation
11	05121	Selected	
12	05261	Selected	
13	06426	Selected	
14	06453	Not Selected	Recording ends after 9 hours 15 minutes
15	06995	Selected	
16	07162	Selected	
17	07859	Selected	
18	07879	Selected	
19	07910	Selected	
20	08215	Selected	
21	08219	Selected	
22	08378	Not Selected	No start time
23	08405	Not Selected	No start time; block 1067 is unreadable
24	08434	Not Selected	Blocks 648, 857 and 894 are unreadable.
25	08455	Not Selected	No start time

In the database the annotations of each file is provided. The annotation of those files is used to compare with proposed framework results and calculate the sensitivity, specificity and accuracy [3.1].

3.2.2 FIR Filter Design

Finite impulse response (FIR) filters are of great importance for multirate systems. The general advantages of FIR systems, inherent system stability and phase linearity, are desirable properties for multirate signal processing. Using multirate techniques, the efficiency of a multirate FIR filter significantly increases in comparison with the single rate implementations. These are the main reasons why most of the practical multirate systems are based on FIR filtering [3.2].

3.2.3 Polyphase Decomposition

Let us consider the discrete sampling of the signal $\{x[n]\}$. The reference time instant for the sampling function $\{s_M[n]\}$ can be shifted from zero to some other time instant k , $0 \leq k \leq M$. Hence, we can define the time-shifted sampling functions $\{s_{M,k}[n]\} = \{s_M[n - k]\}$ with $k = 0, 1, 2, \dots, M - 1$.

$$s_{M,k}[n] = \begin{cases} 1, & n = k, k \pm M, k \pm 2M, \dots, \\ 0, & \text{otherwise} \end{cases} \quad (3.1)$$

In general, for the given $\{x[n]\}$ and M , one can write

$$x[n] = \sum_{k=0}^{M-1} x_k^{(p)}[n] = \sum_{k=0}^{M-1} x[n]s_M[n - k] \quad (3.2)$$

This representation is called the polyphase representation of a discrete signal, or polyphase decomposition. The signal components $\{x_k^{(p)}[n]\}, k = 0, 1, 2, \dots, M - 1$ are called the polyphase components of the signal $\{x[n]\}$.

Polyphase Realization Structures for FIR Filters:

An order top FIR filter can be performed in a parallel structure based on the polyphase decomposition of the transfer function. The transfer function is decomposed into lower order M FIR transfer functions, called multiphase components, and then added to compensate for the total of the original transfer function.

In a general case, an N -length transfer function $H(z)$ can be decomposed into M polyphase branches $E_0(z), E_1(z), \dots, E_{M-1}(z)$ in a manner that $H(z)$ is expressible in the form

$$H(z) = \sum_{k=0}^{M-1} z^{-k} E_k(z^M) \quad (3.3)$$

$$\text{Where, } E_k(z) = \sum_{n=0}^{\lfloor N/M \rfloor} h[Mn + k]z^{-n}, 0 \leq k \leq M - 1 \quad (3.4)$$

The input sequences in the polyphase branches, $\{x_0[m]\}, \{x_1[m]\}, \{x_2[m]\}, \dots, \{x_{(M-1)}[m]\}$ are delayed and down-sampled versions of the input signal $\{x[n]\}$. We can say that the particular sequence $\{x_k[m]\}$ is obtained when down-sampling-by- M the sequence $\{x[n]\}$ with the phase offset $k, k = 0, 1, \dots, M - 1$. Hence, from the causal sequence $\{x[n]\} = \{\dots, 0, 0, x[0], x[1], x[2], \dots, x[M - 1], x[M], x[M + 1], \dots\}$ it is straightforward to extract the M sequences,

$$\{x[n]\} = \{\dots, 0, 0, x[0], x[1], x[2], \dots, x[M - 1], x[M], x[M + 1], \dots\}$$

$$\{x_0[m]\} = \{x[0], x[M], x[2M], \dots\}$$

$$\{x_1[m]\} = \{x[-1], x[M - 1], x[2M - 1], \dots\}$$

$$\{x_2[m]\} = \{x[-2], x[M - 2], x[2M - 2], \dots\}$$

⋮

$$\{x_{M-1}[m]\} = \{x[-M + 1], x[1], x[M + 1], x[2M + 1], \dots\}.$$

Evidently, those sequences can be selected from the input signal $\{x[n]\}$ directly by using the commutative structure with the rotator shown in Figure 3.1.

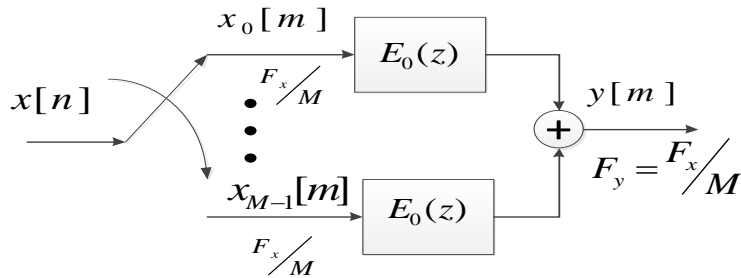


Figure 3. 1: Commutative polyphase structure of an interpolator [3.2].

The rotator initially starts at $n = 0$ and the current sample $x[0]$ is obtained for $E_0(z)$. The next sample $x[1]$, the instantaneous moment $n = 1$, passes $E_{M-1}(z)$. Rotator continues the same shift to the left. Obviously, the rotator works at high speed $\{x[n]\}$, while the poly-phase branch filter is performed at low frequency signal speed $\{y[n]\}$.

Figure 3.2 shows the commutative poly-phase structure of a decimator. The output samples $y[m]$ are obtained sequentially collecting filtered sample samples $\{u_0[n]\}$, $\{u_1[n]\}$, $\{u_2[n]\}$, ..., $\{u_{M-1}[n]\}$, at the output sampling rate

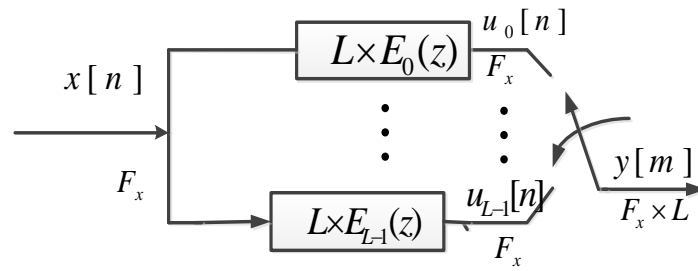


Figure 3. 2: Commutative polyphase structure of a decimator [3.2].

3.2.4 Proposed Multistage Multirate Polyphase Filter

Figure 3.3 shows the general scheme of proposed multistage multirate system design. This system has been used the fractional sampling rate by cascading a factor-of- L interpolator with a factor-of- M decimator, where L and M are positive integer. We have used as $H(z)$ decimation filter and $G(z)$ as interpolation filter. These two filters operate with same or different sampling rate, they can be replaced with a single filter designed to avoid aliasing. The 1st stage and 2nd stage form an analysis filter and synthesis filter with Polyphase branches. Configurations based on Polyphase decomposition are convenient in applications where L and M are small numbers. Otherwise, filters of a very high order are requested. For proposed multistage multirate filter system design is considered three cases which is describe below.

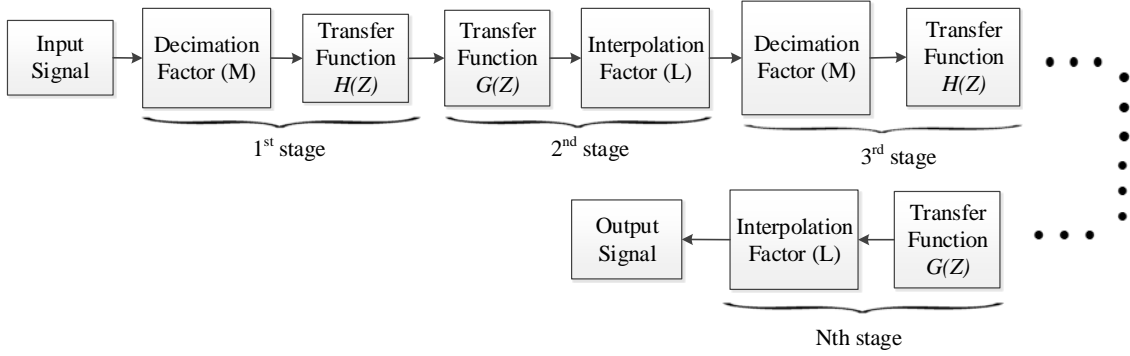


Figure 3. 3: Proposed diagram for multistage implementation of sampling rate alteration system.

Case I:

Consider the proposed design of low-pass FIR filter with poly-phase decomposition and decimation for ECG signals to meet the following specifications:

Parameters	Parameters values
Decimate factor (M)	5
Pass-band edge (ω_p)	0.08π
Stop-band edge (ω_s)	$\frac{2\pi}{M} - \omega_p$
Pass-band ripples (A_p)	40 dB
Stop-bands ripples (A_s)	60 dB

Designing the filter transfer function $H(z)$ by N^{th} order lowpass FIR digital filter from the above specifications and returns the filter coefficients $h[n]$ in length $N + 1$ as shown in Table 3.2 and its frequency response in Figure 3.4 where we take the sampling frequency $f_s = 500\text{Hz}$. The transfer function is formed as

$$H(Z) = h[0] + h[1] z^{-1} + h[2] z^{-2} + h[3] z^{-3} + h[4] z^{-4} + h[5] z^{-5} + h[6] z^{-6} + h[7] z^{-7} + h[8] z^{-8} + h[9] z^{-9} \quad (3.5)$$

Table3. 2: The impulse response $h(n)$ or filter coefficients of frequency sampling filter ($N=9$).

n	$h[n]$	n	$h[n]$
0	-0.0022	9	-0.0022
1	0.0669	8	0.0669
2	0.1097	7	0.1097
3	0.1610	6	0.1610
4	0.1928	5	0.1928

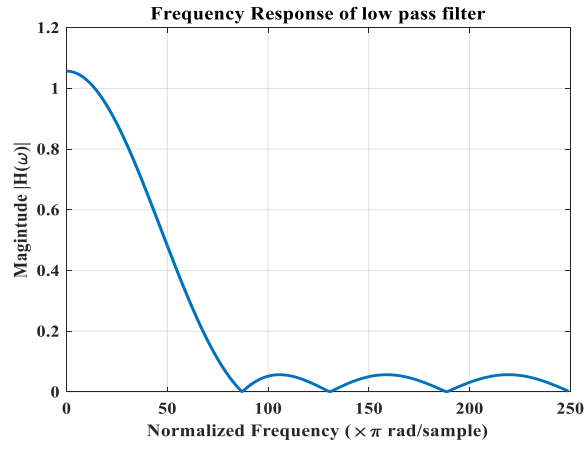


Figure 3. 4: Frequency response of design low pass for FIR filter.

Then performed decomposition of the filter transfer function $H(z)$ into 5 poly-phase components using the equation (3.6).

$$H(z) = E_0(z^5) + z^{-1}E_1(z^5) + z^{-2}E_2(z^5) + z^{-3}E_3(z^5) + z^{-4} E_4(z^5) \quad (3.6)$$

Where,

$$E_0(z) = \{h[0] + h[5] z^{-5}\}$$

$$E_1(z) = \{h[1] + h[6] z^{-5}\}$$

$$E_2(z) = \{h[2] + h[7] z^{-5}\}$$

$$E_3(z) = \{h[3] + h[8] z^{-5}\}$$

$$E_4(z) = \{h[4] + h[9] z^{-5}\}$$

So,

$$H(z) = \sum_{k=0}^{M-1} z^{-k} E_k(z^M) \quad (3.7)$$

$$\text{Where, } E_k(z) = \sum_{n=0}^{\lfloor N/M \rfloor} h[Mn + k] z^{-n}, 0 \leq k \leq M - 1 \quad (3.8)$$

Set decimation-by- $M=5$ for the input signal $x[n]$. In this step, the input $\{x[n]\}$ is decomposed into the set of 5 subsequences: $\{x_0[m]\}, \{x_1[m]\}, \{x_2[m]\}, \{x_3[m]\}, \{x_4[m]\}$. Here, for the causal $\{x[n]\}$ we have $x[-1] = x[-2] = x[-3] = x[-4] = 0$. The 5 subsequences are filtered in the poly-phase branches and added together to give the decimated signal $\{y_{dec}[m]\}$. The realization analysis filter structure of proposed system is shown in Figure 3.5.

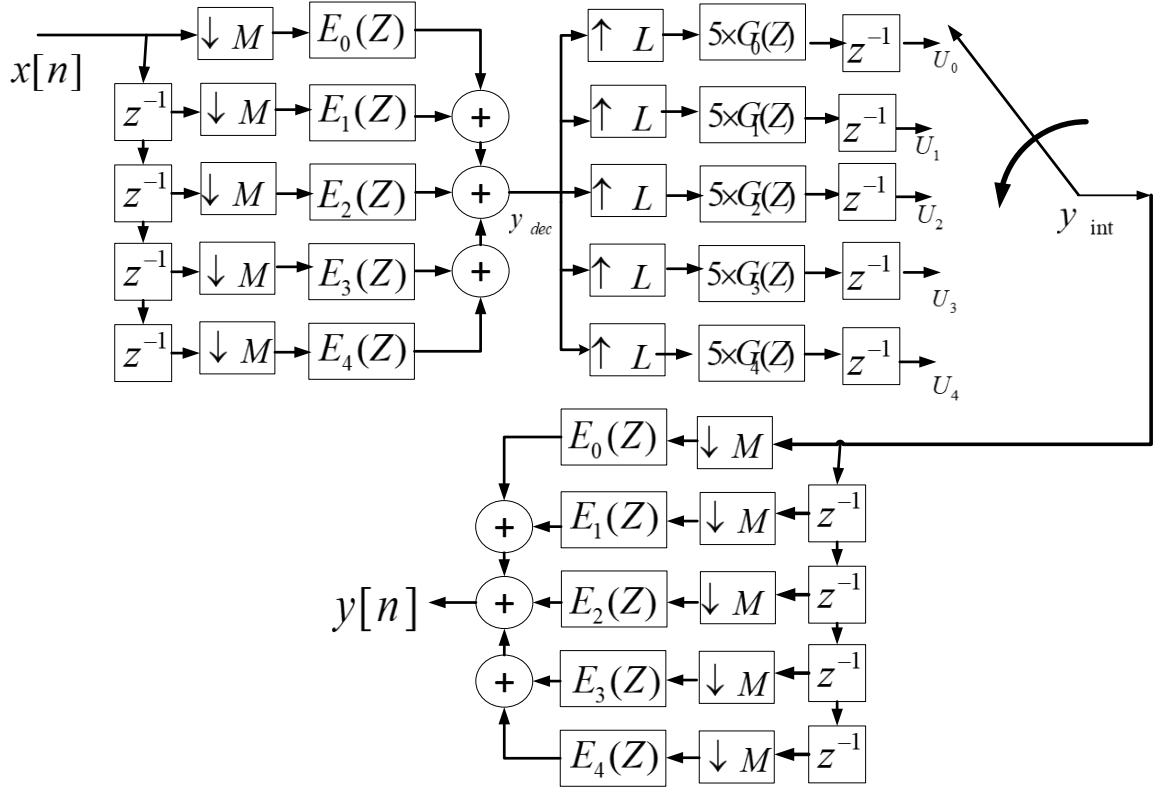


Figure 3. 5: Proposed multistage multirate system for case I.

Choose interpolation-by- $L=5$ into the multistage multirate system structure using polyphase decompose as shown in Figure 3.5. In this step, signal $\{y_{dec}[m]\}$ is used as an input to the interpolator .The signal $\{x[n]\} = \{y_{dec}[m]\}$ is filtered in the parallel poly-phase branches and the set of 5 signals $\{g_0[n]\}, \{g_1[n]\}, \{g_2[n]\}, \{g_4[n]\}, \{g_5[n]\}$, is obtained as the equations (3.9)-(3.13) . The matrix G is composed of 5 row vectors: $\{g_0[n]\}, \{g_1[n]\}, \{g_2[n]\}, \{g_3[n]\}, \{g_4[n]\}$. The samples of the interpolated signal $\{y_{int}[m]\}$ are stored column-wise in matrix U . The interpolated signal considered as a synthesis filter is obtained simply by picking up the samples from matrix U .

$$g_0(n) = \{h[0]y_{dec}(n) + h[5]y_{dec}(n - 1)\} \quad (3.9)$$

$$g_1(n) = \{h[1]y_{dec}(n) + h[6]y_{dec}(n - 1)\} \quad (3.10)$$

$$g_2(n) = \{h[2]y_{\text{dec}}(n) + h[7]y_{\text{dec}}(n - 1)\} \quad (3.11)$$

$$g_3(n) = \{h[3]y_{\text{dec}}(n) + h[8]y_{\text{dec}}(n - 1)\} \quad (3.12)$$

$$g_4(n) = \{h[4]y_{\text{dec}}(n) + h[9]y_{\text{dec}}(n - 1)\} \quad (3.13)$$

Taking inverse Z-transform of the equations (3.9) to (3.13), is obtained as

$$G_0(z) = \{h[0]Y[z] + h[5]z^{-1}Y[z]\} \quad (3.14)$$

$$G_1(z) = \{h[1]Y[z] + h[6]z^{-1}Y[z]\} \quad (3.15)$$

$$G_2(z) = \{h[2]Y[z] + h[7]z^{-1}Y[z]\} \quad (3.16)$$

$$G_3(z) = \{h[3]Y[z] + h[8]z^{-1}Y[z]\} \quad (3.17)$$

$$G_4(z) = \{h[4]Y[z] + h[9]z^{-1}Y[z]\} \quad (3.18)$$

For multistage purpose, further we have decimated y_{int} by $M=5$ with the equation (3.6) or follow the procedures of 1st stage structure.

Case II:

In case II, we considered a N^{th} order low-pass digital FIR filter with poly-phase decomposition and decimation/interpolation for biomedical signals to meet the following specifications:

Parameters	Parameters values
Decimate factor (M)	5
Filter order, N	81
Cut-off frequency	1/M

Table3. 3: The impulse response h(n) or filter coefficients of frequency sampling filter (N=81).

n	h(n)	n	h(n)	n	h(n)	n	h(n)
0	0.00019	21	-0.00286	42	0.17140	63	0.00652
1	-0.00020	22	-0.00840	43	0.12641	64	0.00467
2	-0.00057	23	-0.01161	44	0.07245	65	0.00157
3	-0.00079	24	-0.01050	45	0.02128	66	-0.00138
4	-0.00072	25	-0.00448	46	-0.01717	67	-0.00317
5	-0.00032	26	0.00502	47	-0.03741	68	-0.00342
6	0.00037	27	0.01471	48	-0.03929	69	-0.00240
7	0.00113	28	0.02041	49	-0.02742	70	-0.00079
8	0.00163	29	0.01859	50	-0.00913	71	0.00068
9	0.00154	30	0.00803	51	0.00803	72	0.00154
10	0.00068	31	-0.00913	52	0.01859	73	0.00163
11	-0.00079	32	-0.02742	53	0.02041	74	0.00113
12	-0.00240	33	-0.03929	54	0.01471	75	0.00037
13	-0.00342	34	-0.03741	55	0.00502	76	-0.00032
14	-0.00317	35	-0.01717	56	-0.00448	77	-0.00072
15	-0.00138	36	0.02128	57	-0.01050	78	-0.00079
16	0.00157	37	0.07245	58	-0.01161	79	-0.00057
17	0.00467	38	0.12641	59	-0.00840	80	-0.00020
18	0.00652	39	0.17140	60	-0.00286	81	0.00019
19	0.00594	40	0.19695	61	0.00255	-	-
20	0.00255	41	0.19695	62	0.00594	-	-

From the above sections we found the transfer function $H(z)$ by N^{th} order lowpass FIR digital filter and filter coefficients $h[n]$ in length $N+1$ as shown in Table 3.3. Its frequency response in Figure 3.6 where $f_s=500\text{Hz}$. The transfer function is formed as

$$H[z] = h[0] + h[1] z^{-1} + h[2]z^{-2} + \dots + h[81]z^{-81} \quad (3.19)$$

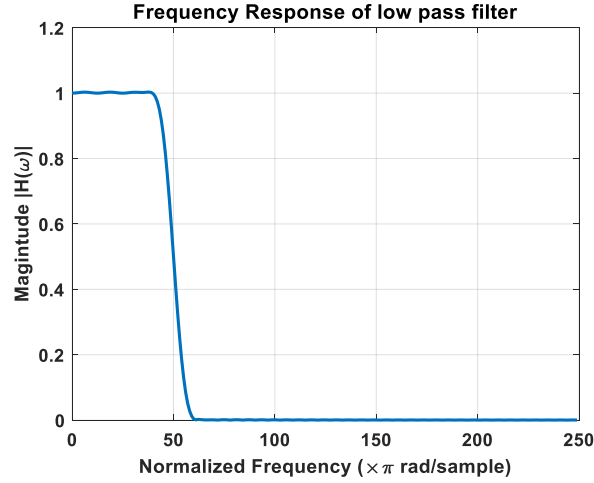


Figure 3. 6: Frequency response of design low pass for FIR filter.

Then performed decomposition of the filter transfer function $H(z)$ into 2 poly-phase components using the equation (3.19).

$$H(z) = E_0(z^2) + z^{-1}E_1(z^2) \quad (3.20)$$

Where,

$$E_0 = h[0] + h[2]z^{-2} + h[4]z^{-4} + \dots + h[80]z^{-80}$$

$$E_1 = h[1]z^{-1} + h[3]z^{-3} + h[5]z^{-5} + \dots + h[81]z^{-80}$$

$$E_{00} = h[0] + h[6]z^{-6} + h[12]z^{-12} + \dots + h[78]z^{-78}$$

$$E_{01} = h[2]z^{-2} + h[8]z^{-8} + h[14]z^{-14} + \dots + h[80]z^{-80}$$

$$E_{02} = h[4]z^{-4} + h[10]z^{-10} + h[16]z^{-16} + \dots + h[76]z^{-76}$$

$$E_{10} = h[1]z^{-1} + h[7]z^{-7} + h[13]z^{-13} + \dots + h[79]z^{-79}$$

$$E_{11} = h[3]z^{-3} + h[9]z^{-9} + h[15]z^{-15} + \dots + h[81]z^{-81}$$

$$E_{12} = h[5]z^{-5} + h[11]z^{-11} + h[17]z^{-17} + \dots + h[77]z^{-77}$$

Decimated-by- $M=2$. In this step, the input $\{x[n]\}$ is break down into the set of 2 subsequences: $\{x_0[m]\}$, $\{x_1[m]\}$. Here, for the causal $\{x[n]\}$ we have $x[-1] = x[-2] = 0$. The 2 subsequences are interpolated by 3 in the poly-phase branches and added together to give the decimated signal $\{y_{\text{dec}}[m]\}$. The actualization analysis filter structure of proposed system is shown in Figure 3.7.

For multistage purpose, further we have up-sampled & down-sampled the decimated signal $\{y_{dec} [m]\}$ is down-sampled by $M=10$ then up-sampled by $L=10$.

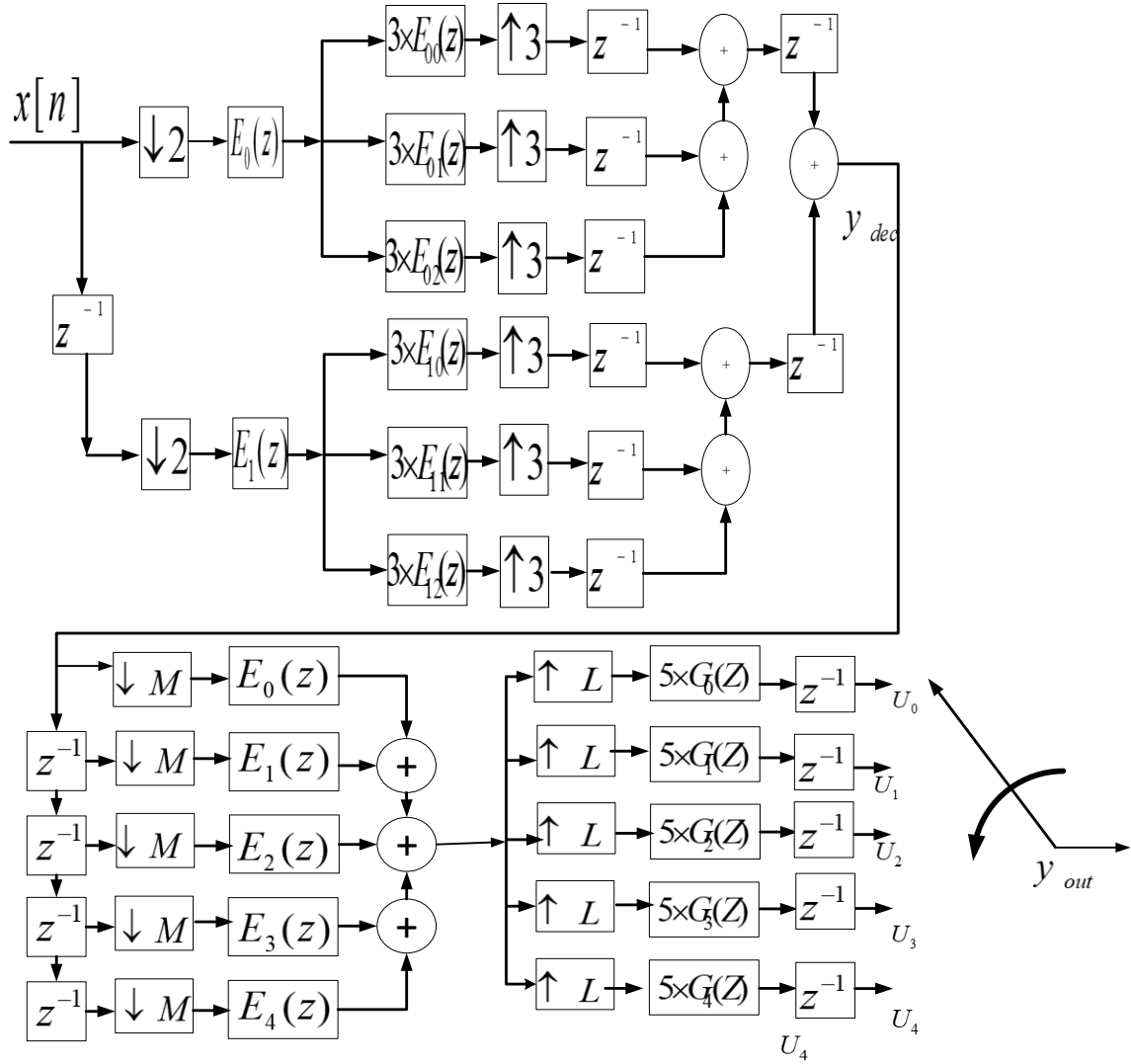


Figure 3. 7: Proposed multistage multirate system for case II.

Case III:

Consider the design specification of case II, the decimated signal $\{y_{dec} [m]\}$ of case II is used as an input to the interpolator and interpolated by $L=2$, then the 2 subsequences are decimated by 3 in the poly-phase branches and added together to give the interpolated signal $\{y_{int} [m]\}$. The fulfillment analysis filter structure of proposed system is shown in Figure 3.8.

The signal $\{x[n]\} = \{y_{\text{dec}}[m]\}$ is filtered in the parallel poly-phase branches and the set of 2 signals $\{g_0[n]\}, \{g_1[n]\}$ and the subsequences of this two signals $\{g_{00}[n]\}, \{g_{01}[n]\}, \{g_{02}[n]\}, \{g_{10}[n]\}, \{g_{11}[n]\}, \{g_{12}[n]\}$ is obtained as the equations (3.22)-(3.29) and added together to give the interpolated signal $\{y_{\text{int}}[m]\}$.

$$\{g_0[n]\} = \{g[0], g[M], g[2M], \dots\}$$

$$\{g_1[n]\} = \{g[-1], g[M-1], g[2M-1], \dots\}$$

$$\{g_2[n]\} = \{g[-2], g[M-2], g[2M-2], \dots\}$$

⋮

$$\{g_{M-1}[n]\} = \{g[-M+1], g[1], g[M+1], g[2M+1], \dots\}. \quad (3.21)$$

Where the equation can be represented based on the design specifications as,

$$g_0[n] = h[0]y_{\text{dec}}[n] + h[2]y_{\text{dec}}[n-1] + h[4]y_{\text{dec}}[n-2] + \dots + h[80]y_{\text{dec}}[n-40] \quad (3.22)$$

$$g_1[n] = h[1]y_{\text{dec}}[n] + h[3]y_{\text{dec}}[n-1] + h[5]y_{\text{dec}}[n-2] + \dots + h[81]y_{\text{dec}}[n-40] \quad (3.23)$$

$$g_{00}[n] = h[0]y_{\text{dec}}[n] + h[6]y_{\text{dec}}[n-3] + h[12]y_{\text{dec}}[n-6] + \dots + h[78]y_{\text{dec}}[n-39] \quad (3.24)$$

$$g_{01}[n] = h[2]y_{\text{dec}}[n-1] + h[8]y_{\text{dec}}[n-4] + h[14]y_{\text{dec}}[n-7] + \dots + h[80]y_{\text{dec}}[n-40] \quad (3.25)$$

$$g_{02}[n] = h[4]y_{\text{dec}}[n-2] + h[10]y_{\text{dec}}[n-5] + h[16]y_{\text{dec}}[n-8] + \dots + h[76]y_{\text{dec}}[n-38] \quad (3.26)$$

$$g_{10}[n] = h[1]y_{\text{dec}}[n] + h[7]y_{\text{dec}}[n-3] + h[13]y_{\text{dec}}[n-6] + \dots + h[79]y_{\text{dec}}[n-39] \quad (3.27)$$

$$g_{11}[n] = h[3]y_{\text{dec}}[n-1] + h[9]y_{\text{dec}}[n-4] + h[15]y_{\text{dec}}[n-7] + \dots + h[81]y_{\text{dec}}[n-40] \quad (3.28)$$

$$g_{12}[n] = h[5]y_{\text{dec}}[n-2] + h[11]y_{\text{dec}}[n-5] + h[17]y_{\text{dec}}[n-8] + \dots + h[77]y_{\text{dec}}[n-38] \quad (3.29)$$

Taking inverse Z-transform of the equations (3.22) to (3.29), is obtained as

$$G_0[z] = h[0]Y[z] + h[2]z^{-1}Y[z] + h[4]z^{-2}Y[z] + \dots + h[80]z^{-40}Y[z] \quad (3.30)$$

$$G_1[z] = h[1]Y[z] + h[3]z^{-1}Y[z] + h[5]z^{-2}Y[z] + \dots + h[81]z^{-40}Y[z] \quad (3.31)$$

$$G_{00}[z] = h[0]Y[z] + h[6]z^{-3}Y[z] + h[12]z^{-6}Y[z] + \dots + h[78]z^{-39}Y[z] \quad (3.32)$$

$$G_{01}[z] = h[2]z^{-1}Y[z] + h[8]z^{-4}Y[z] + h[14]z^{-7}Y[z] + \dots + h[80]z^{-40}Y[z] \quad (3.33)$$

$$G_{02}[z] = h[4]z^{-2}Y[z] + h[10]z^{-5}Y[z] + h[16]z^{-8}Y[z] + \dots + h[76]z^{-38}Y[z] \quad (3.34)$$

$$G_{10}[z] = h[1]Y[z] + h[7]z^{-3}Y[z] + h[13]z^{-6}Y[z] + \dots + h[79]z^{-39}Y[z] \quad (3.35)$$

$$G_{11}[z] = h[3]z^{-1}Y[z] + h[9]z^{-4}Y[z] + h[15]z^{-7}Y[z] + \dots + h[81]z^{-40}Y[z] \quad (3.36)$$

$$G_{12}[z] = h[5]z^{-2}Y[z] + h[11]z^{-5}Y[z] + h[17]z^{-8}Y[z] + \dots + h[77]z^{-38}Y[z] \quad (3.37)$$

For multistage purpose, again the interpolated signal $\{y_{\text{int}}[m]\}$ is decimate-by- $M=2$ and 2 subsequences are interpolated by 3 in the poly-phase branches as a synthesis filter and added together to give the signal $y_{\text{out}}[m]$.

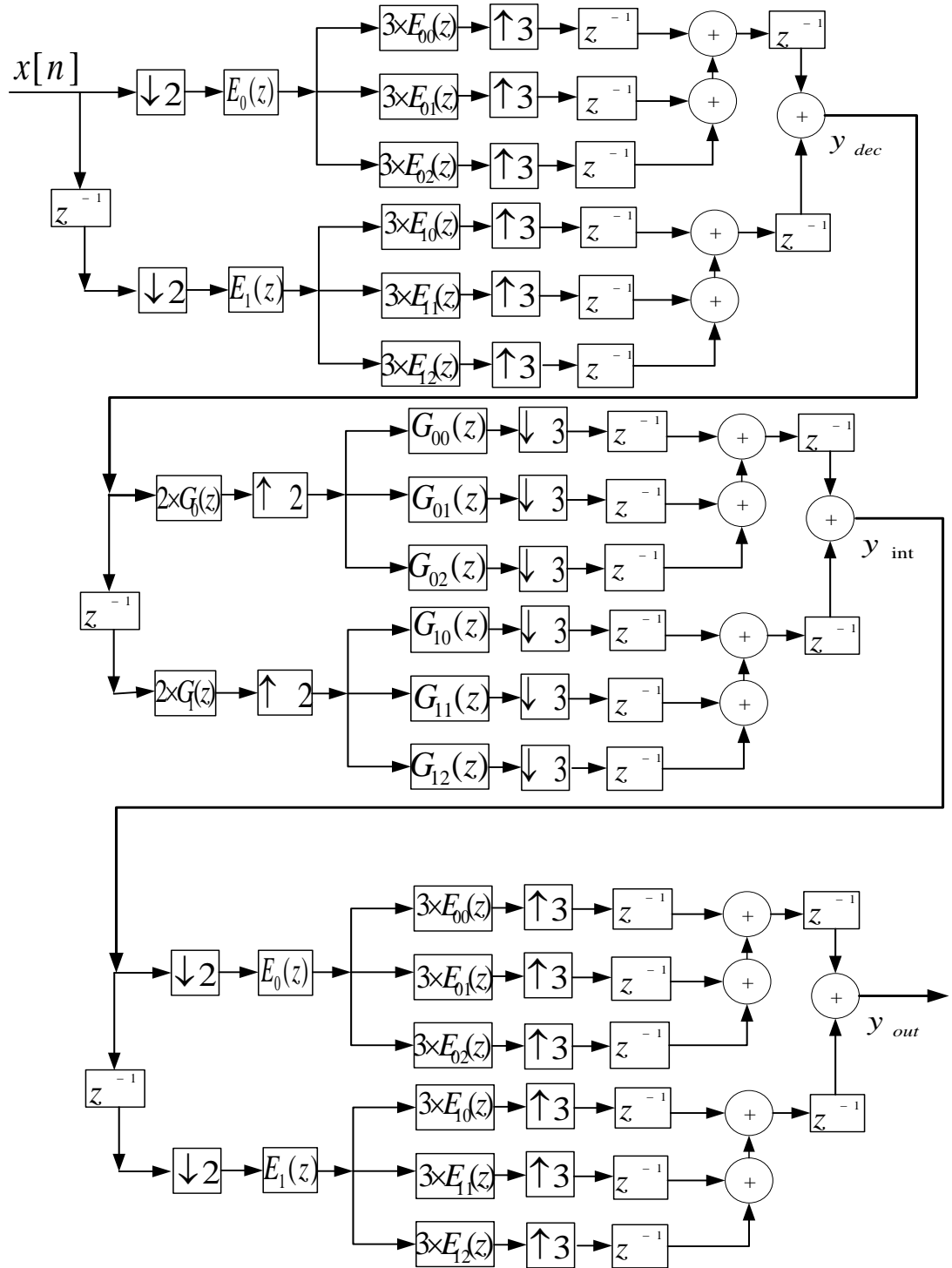


Figure 3. 8: Proposed multistage multirate system for case III.

3.3 Results and Discussion

Figures 3.9 to 3.14 shows the result of proposed multistage multirate system using ECG signals for case I-III as considered in this thesis. All cases use multirate filter specification as shown in Table 3.1 to 3.2 on multistage multirate system to remove noise from ECG data.

We have consider 1st stage as analysis and 2nd stage as synthesis filtering part is performed in multirate system. For multistage operation, we considered repetition process.

Figure 3.9, 3.11 & 3.13 show the original output of all stages with respect to their sampling rate without bit loss for case I-III. The number of bits is equal for all stages.

For case I, proposed multistage multirate system is considered multirate poly-phase decomposition with decimation and interpolation. The sampling rate conversion factor is considered by down sampling factor $M=5$, up sampling factor $L=5$ and filter order $N=9$ for case I. Left side of colume in Figure 3.10, 3.12, & 3.14 (a) shows the zoom in output, smooth ECG signal with three different stages of propsoed multistage multirate system for case I-III and compared with wavelet 9/7 [3.3], [3.4] and their perspective frequency histogram. Figure 3.10 (a), shows better smooth signal where sampling rate is down by $M=5$ in 1st stage and the 2nd stage increases the sampling rata by $L=5$ into the multirate Polyphase filter. For better performance again apply 3rd stage as analyses filter and got smooth signal than 2nd stage as shown in Figure 3.10 (a) that's helps to detect R peak. For comparison of proposed system and wavelet 9/7, we have used histogram analysis and autocorrelation function. Right side column of Figure 3.10(a) shows the frequency distribution of noisy ECG signal, smoothed signal by proposed system and wavelet 9/7 for case I. The proposed systems have shown better frequency distribution shape where positions are slight because of sampling rate increases or decreases in the system as compared with wavelet 9/7.

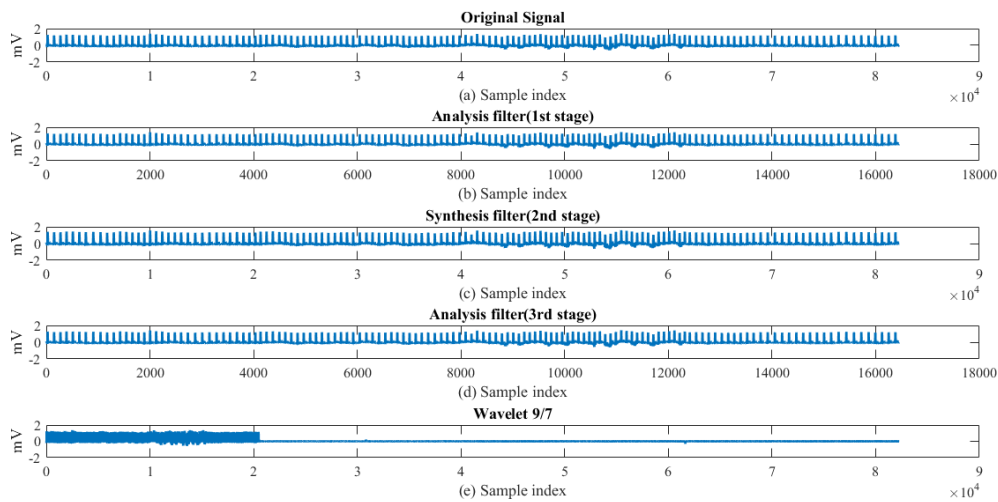


Figure 3. 9: Multistage filtering of noisy ECG signal (MIT BIH AF 08215m.mat) for case I.

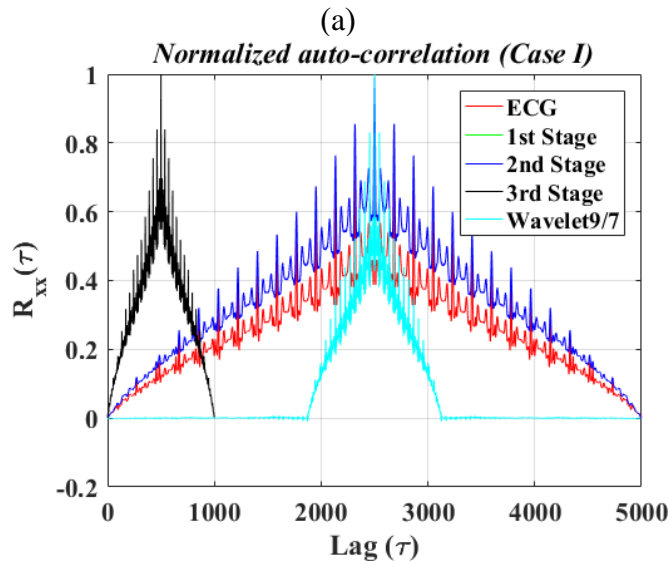
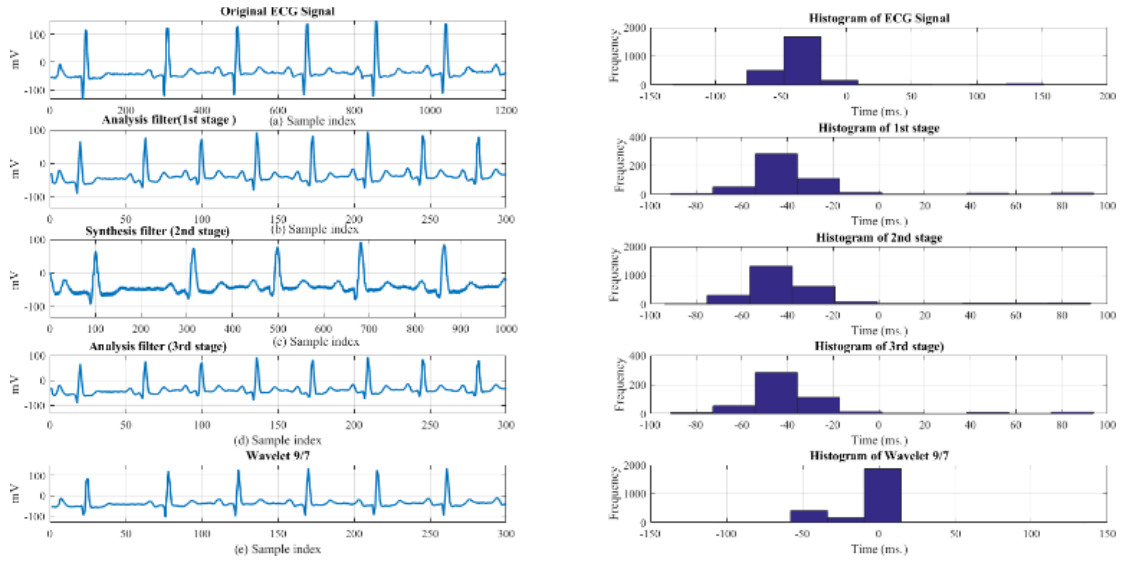


Figure 3. 10: (a) Multistage filtering of noisy ECG signal (MIT BIH AF 08215m.mat) zoom in part & Frequency response (b) Normalized Autocorrelation for Case I.

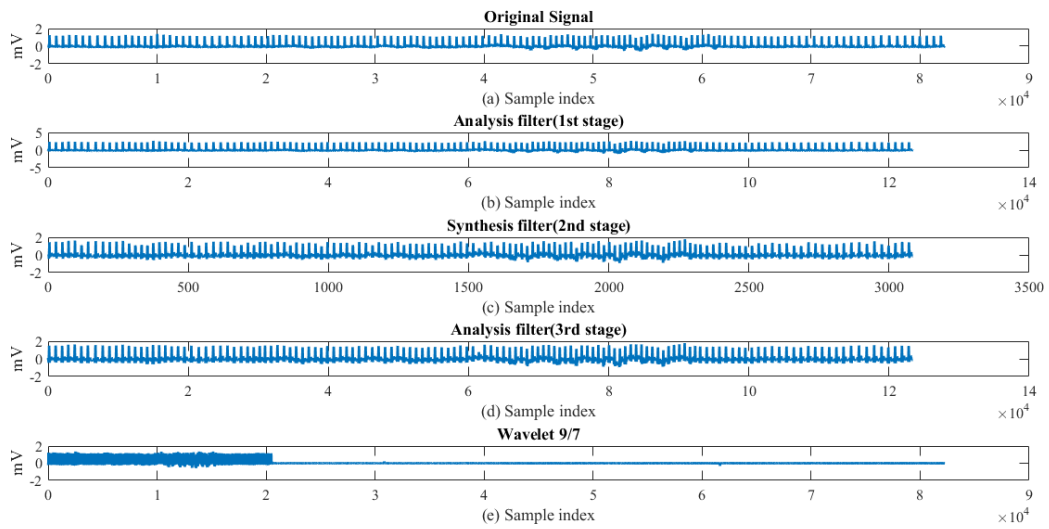
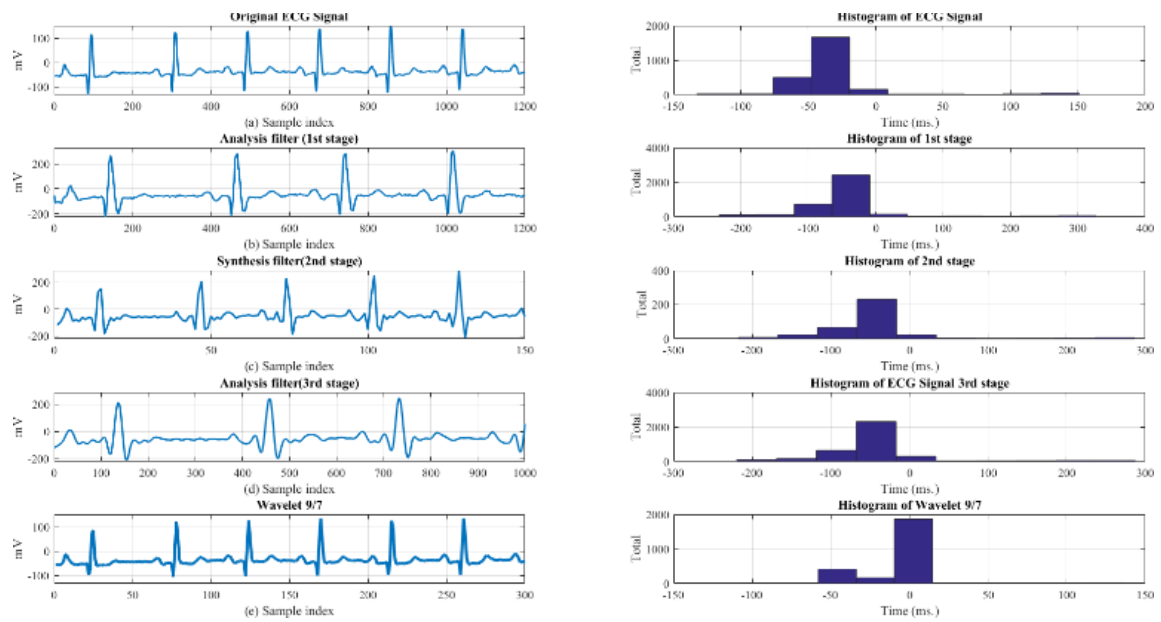
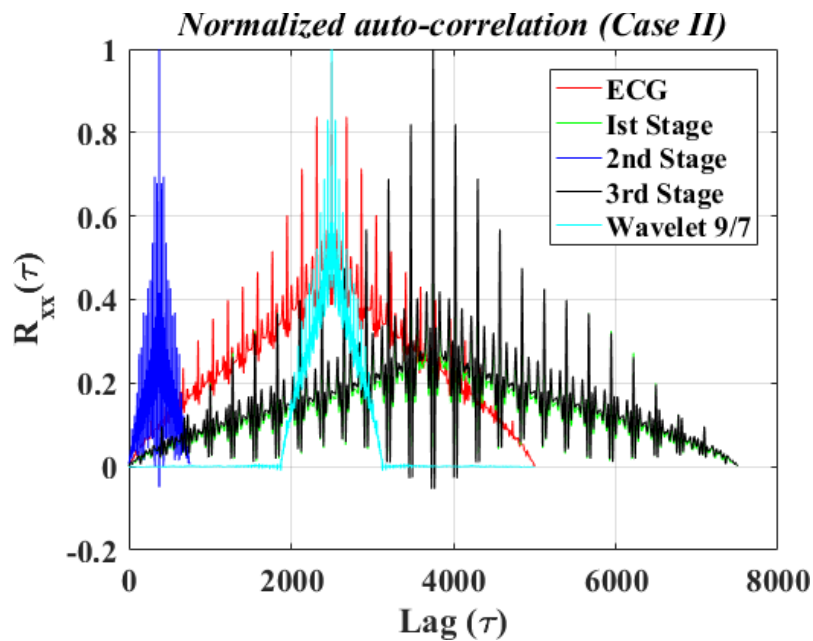


Figure 3. 11: Multistage filtering of noisy ECG signal for case II.



(a)



(b)

Figure 3.12: (a) Multistage filtering of noisy ECG signal (MIT BIH AF 08215m.mat) zoom in part & Frequency response (b) Normalized Autocorrelation for Case II.

On the other sides in Figure 3.10 (b) shows comparison based on autocorrelations for case I. For Case II, the sampling rate conversion factor is considered by filter order $N=81$. Figure 3.12 (a), sampling rate is taken for rational sampling factor $L/M=3/2$ of ECG signals in the analysis filtering part, and show better signal than noisy signal. On the other side, synthesis filter decreases the sampling rata by $M= 10$, and get better signal than analyzed signal (1st stage) as shown in the Figures 3.12 (a). For better performance again apply analyses filtering

by $L=10$ on that synthesis filtered signal and got smooth signal than 2nd stage as shown in Figure 3.12 (a) that's helps to detect R peak easily. For Case III, in the analysis filtering (1st stage) part, sampling rate increased because of rational sampling factor $L/M=3/2$. The performance between analysis filter and synthesis filter is also increases the sampling rate $L/M=2/3$ and gave better result than 1st stage as shown in the Figure 14(a). For better performance apply the output of the 2nd stage into the synthesis filtered (3rd stage) where the sampling rate was $L/M=3/2$. The results showed smooth signal than 2nd stage that's helps to detect R peak easily.

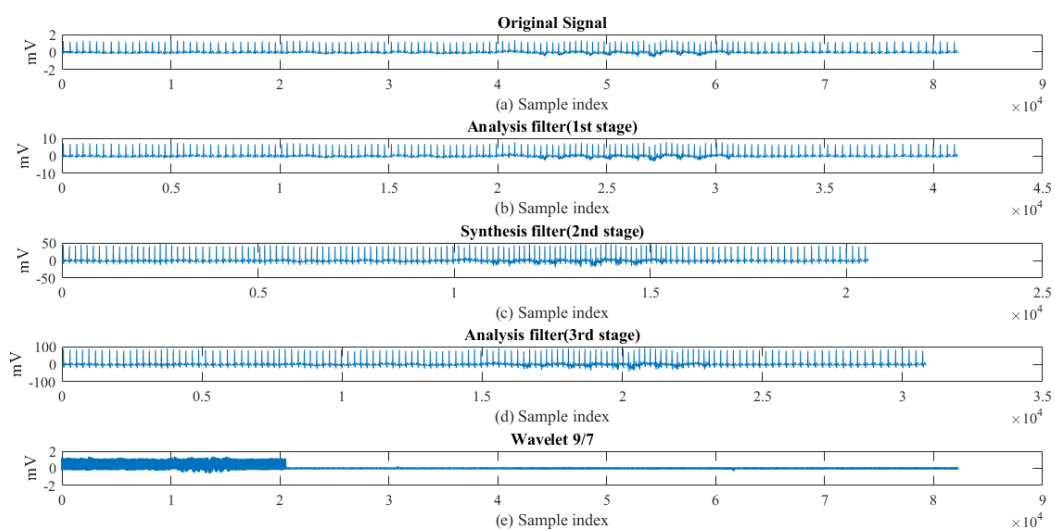
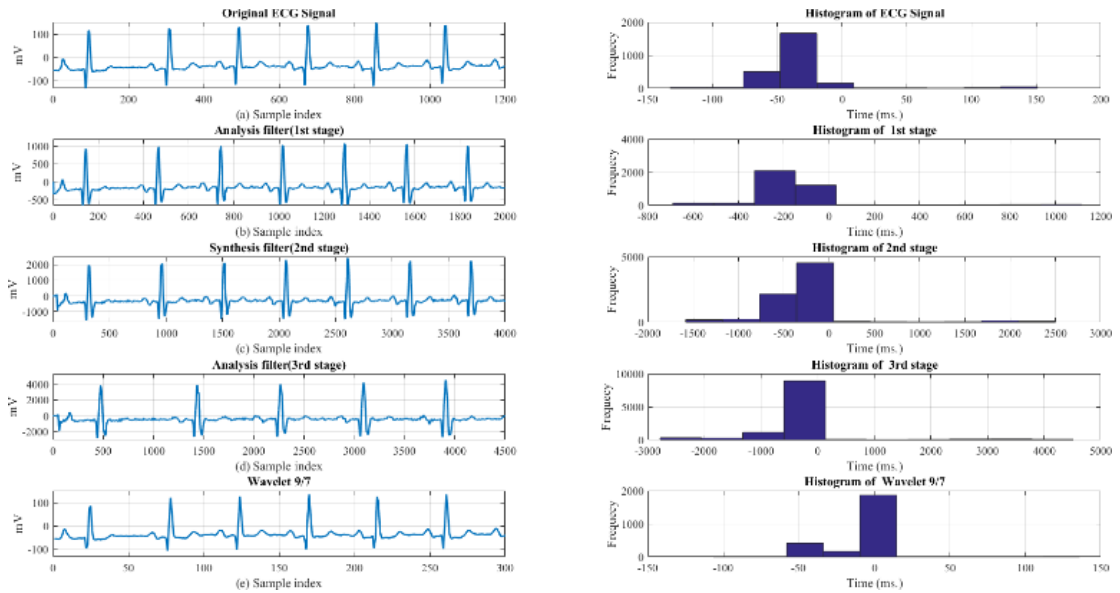
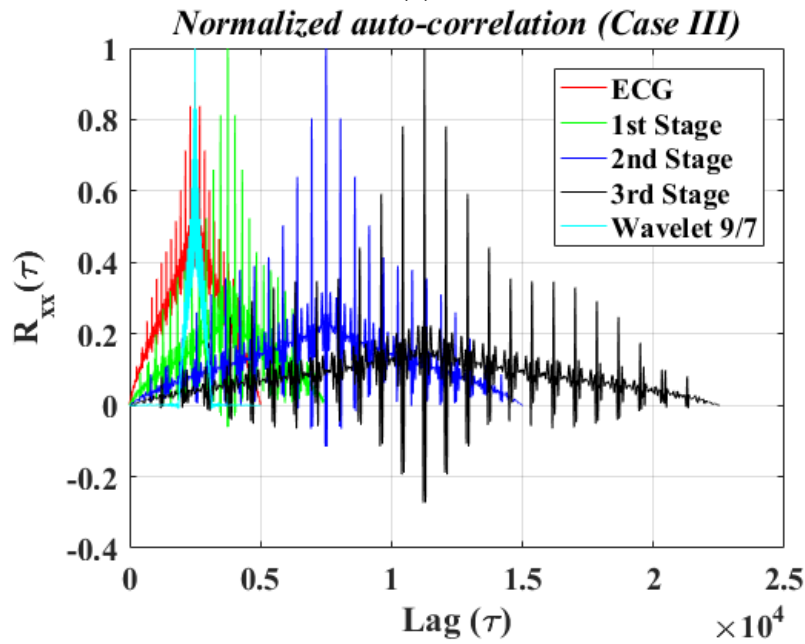


Figure 3. 13: Multistage filtering of noisy ECG signal (MIT BIH AF 08215m.mat) for case III.



(a)



(b)

Figure 3. 14: (a) Multistage filtering of noisy ECG signal (MIT BIH AF 08215m.mat) zoom in part & Frequency response (b) Normalized Autocorrelation for Case III.

From the histogram of figure 3.10, 3.12 & 3.14 (a) for case I-III, it also shown that stages 1st-3rd has different frequency density with respect to their frequency distribution for various sampling rate and compared with wavelet 9/7. The histogram of 1st stage to 3rd stage rates is bell-shaped with one peak for all case. There are no gaps or extreme values. So, proposed systems give better results than wavelet 9/7 systems for every case.

Now briefly justify histogram for only case I, 1st stage has a maximum value of 90 and a minimum value of -85 with one peak between -35 and -60. 2nd stage has a maximum value of 90 and a minimum value of -85, one peak between -35 and -60. 3rd stage has a maximum value of 90 and a minimum value of -85 with one peak between -35 and -60. The wavelet 9/7 has skew left in the frequency distribution where a maximum value of 140 and a minimum value of -110 with one peak between 18 and -12. Such as case II & case III also show better smooth ECG signal for 1st to 3rd stage than wavelet 9/7.

For comparison between the ECG signal and proposed system, also considered autocorrelation processes for robustness of algorithms. Figure 3.10-3.12 (b), the representation of auto correlation values of ECG signal as red color, 1st, 2nd, 3rd stage as green, blue black color and wavelet 9/7 as cyan color. The results of cases I-III with three different stages show high peaks and good correlated values with different sampling rate. There are no data loss that's why there are no unusual patterns in our graphical representation but position shift for various sampling rate. Figure 3.10(b) for case I, it also observed that the autocorrelation of 1st and 3rd stage overlap to each other because the output of 1st stage is applied to the 2nd stage. Then the output of 2nd stage is applied to the 3rd stage and finally the L/M is same for 1st & 3rd stage that's why their frequency distribution also same for same sampling rate.

3.4 Summary

Multistage multirate system have been proposed for removing noise, requiring low-cost and equal or fractional sampling rates for ECG signal processing. This system has considered three case for better justification of proposed system with sampling rate conversion. From the results analysis it can be concluded that all cases show better quality of ECG signal with the effect of reduce/increase the sample values of noisy ECG signals. These algorithms can be more efficient for diagnosis purpose. In future more, multistage methodology should be developed for biomedical applications to get more accurate performance.

The next chapter will cover the methodologies, proposed algorithms, result, discussion and summary of AF detection from ECG signal.

REFERENCES

- [3.1] MIT-BIH Atrial Fibrillation Database:
<http://physionet.org/physiobank/database/afdb>
- [3.2] L. Milić, “Multirate Filtering for Digital Signal Processing, MATLAB Applications”, *Ljiljana Milić Pub.* Chapter 2-4, pp 23-111.
- [3.3] I. Daubechies, W. Sweldens, “Factoring Wavelet Transforms into Lifting Steps,” *J. Fourier Anal. Appl.*, vol. 4, no. 3, pp. 247 – 269, May 1998.
- [3.4] Z. Guangjun, C. Lizhi and C. Huowang, “A simple 9/7-tap wavelet filter based on lifting scheme”, *Proceedings 2001 International Conference on Image Processing (Cat. No.01CH37205)*, vol. 2, pp. 249 – 252, 2001.
- [3.5] R. E. Crochiere and L. R. Rabiner, “Multirate Digital Signal Processing”, Publisher: *Pearson; 1st edition*, ISBN-13: 978-0136051626, March 21, 1983.
- [3.6] P. P. Vaidyanathan, “Multirate System and Filter Banks”, *Publisher: Prentice Hall; 1 edition*, ISBN-13: 978-0136057185, October 1, 1992.
- [3.7] R.G. Shenoy, D. Burnside and T.W. Parks, “Linear Periodic Systems and Multirate Filter Design”, *IEEE Transactions on Signal Processing*, vol. 42, Issue: 9, pp.2242 – 2256, September 1994.
- [3.8] G. A. Williamson, S. Dasgupta and F. Minyue, “Multistage Multirate Adaptive Filters”, *IEEE International Conference on Acoustic, Speech, and Signal Processing conference Proceedings*, vol. 3, pp. 1534–1537, 1999.
- [3.9] E. Ifeachor and B. W. Q. Jervis, “Digital Signal Processing: A Practical Approach, 2/E” Publisher”, *Pearson Education India*, ISBN 813708241, 9788131708248, 2002.
- [3.10] E. Niedermeyer, F. H. L. Silva, “Electroencephalography: Basic Principles, Clinical Applications, and Related Fields”, *Lippincott Williams & Wilkins*, Fifth edition 2005.
- [3.11] Z. Qingju and L. Zhizeng, “Wavelet De-Noising of Electromyography”, *2006 International Conference on Mechatronics and Automation*, Luoyang, Henan, pp. 1553-1558 ,2006.
- [3.12] M. S. Reddy, R. M. Kumar, K. P. Chander and K. S. Rao, “Complex wavelet transform driven de-noising method for an EOG signals”, *2011 Annual IEEE India Conference*, Hyderabad, pp. 1-5, 2011.

- [3.13] O. Shea, Peter, Sadik, Z. Amin, Hussain and, M. N. Zahir, “Digital Signal Processing: An Introduction with MATLAB and Applications”, *Springer Berlin Heidelberg, Berlin, Heidelberg*, pp. 209--227, ISBN:978-3-642-15591-8, 2011.
- [3.14] V. Pandey and V.K. Giri, “High Frequency Noise Removal from ECG using Moving Average Filters”, *International Conference on Emerging Trends in Electrical, Electronics and Sustainable Energy Systems (ICETEESES–16)*, 06 October 2016.

CHAPTER IV

Atrial Fibrillation Detection

Chapter Outlines

- Introduction
- Materials and Methods
- Results and Discussion
- Summary
- References

CHAPTER IV

Atrial Fibrillation Detection

4.1 Introduction

Cardiac arrhythmias are caused by abnormal electrical activity of the heart. Atrial Fibrillation (AF) is one of the most common types of cardiac arrhythmias [4.1]. AF is the most common cardiac arrhythmia found in clinical practice with increased prevalence in the ageing population [4.2]. It affects 5% of those aged over 65 years and 10% of those aged over 80 years [4.2]. Its occurrence is increasing primarily for two reasons; (i) an increase in the ageing population, and (ii) advances in medical care leading to survival from underlying conditions closely associated with AF, such as hypertension, coronary heart disease, and cardiac failure [4.2]. AF is characterized by uncoordinated atrial activation due to disrupted electrical pathways and structural changes in the heart [4.3]. Because of those conditions, AF has come with an increased rate of hospitalizations and medical care. It also has a huge economic impact. It has been described as epidemic in proportion since some researchers have predicted its prevalence will triple by 2050 [4.2]. So, if the AF is detected early then it could reduce the cost of treatment, rate of hospitalization and other risk factor associating with it.

During AF, electrical discharges conducted from the atrium into the ventricles are irregular and as a result, the heart rate becomes irregular and, usually rapid and also the electrical Atrial Activity (AA) is disorganized [4.4]. Both of these characteristics can be easily detected by the analysis of an ECG signal by noticing the irregularity of R-R intervals and the absence of the P-wave [4.5]. So, there are basically two methods for the detection of AF from the ECG signal. They are the RR Irregularity (RRI) and the AA. Any one of the two methods can be followed to detect the AF. The combination of the RR Irregularity and the AA can also be used to get enhanced detection performance. The RR irregularity is the most common method and very frequently used. This method is much easier because the R wave is the most prominent characteristics in the ECG signal, so it is relatively easy to detect. In this thesis, only the RR Irregularity is used to detect the AF from an ECG signal.

The R wave is the most prominent characteristic within the ECG, making it relatively simple to detect. Therefore, algorithms that detect AF based on RRI are the most common in the literature. Five algorithms based on RRI are selected to realize: Moody et al. [4.5], based on Markov Models (MM); Logan et al. [4.6] using a simple variance parameter; Linker et al. [4.7], that used a statistical framework combination; Tatento et al. [4.8], which applied Kolmogorov Smirnov test; and Cerutti et al. [4.9], which used an autoregressive modeling and compares RRI with white noise.

This chapter is organized as follows. A brief description on materials and methods based on proposed framework is given in section 4.2. In section 4.3, obtained results are analyzed and consequent issues are discussed. Finally conclusions are described in section 4.4.

4.2 Materials and Methods

4.2.1 Database

This chapter also use the same database that given in chapter III.

4.2.2 Software and Proposed Algorithm

We have chosen MATLAB R2016a as the software platform to simulate all the programs. MATLAB is a commercial software product, which is available from the Math works. It consists of main ‘engine’ having strong mathematical function built-in which perform the computational and other extended-function libraries for special purpose applications [4.10]. The MATLAB software provides a variety of functions that make it easy and flexible while simulation for interactive designing, advance analyzing, exploration and visualizing signals, filters and windows. It provides the tools for finite impulse response (FIR) and infinite impulse response (IIR), digital filter design, implementation and analysis. It also provides the toolbox for application, such as, Signal Processing Toolbox [4.11], [4.12].

MATLAB has set of constructs for plotting scientific graphs from raw or computed data [4.10]. It is a high-performance language, most productive development and interactive environment for engineering and technology implementations software package. MATLAB enables to perform different functions which includes, electronic programming, technical computing applications, scientific and engineering graphical illustration, accurate numerical

calculation, algorithms development, application development including graphical user interface building, graph and report or software simulation etc. [4.11], [4.12].

In MATLAB we build a program to read the data from the MIT-BIH Atrial Fibrillation database. The data was downloaded from the database at .mat format using the physio net toolbox which is used for data conversion into .mat file [4.13]. Then another program is made to build the signal of RR interval against the number of beats. Then the MATLAB is again used to build a program for AF detection. The MATLAB is also used for the verification of the parameters, such as sensitivity, specificity and accuracy. The total process is described in Fig 4.1.

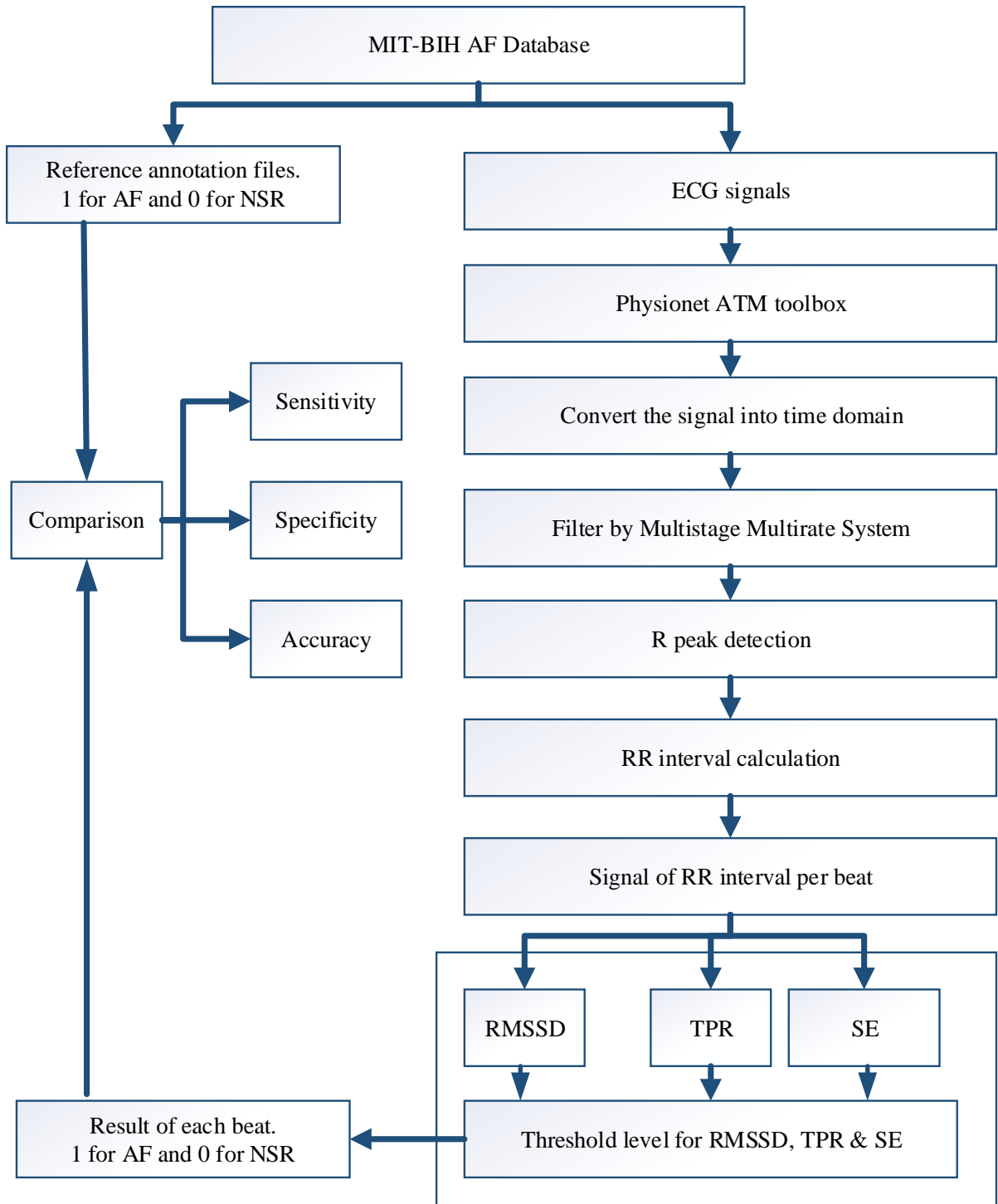


Figure 4. 1: Proposed flowchart, which shows the total process of detecting AF.

This proposed algorithm work flows are described as:

Step 1: Import original ECG signal from MIT-BIH database using Physionet ATM Toolbox.

Step 2: Remove the baseline noise using multistage multirate system.

Step 3: Represent the original ECG signal in time domain by using inverse fast Fourier transform.

Step 4: Detect the peaks of R waves.

Step 5: Calculate the RR interval and plot the signal of RR interval against per beat.

Step 6: Calculate the RMSSD, SE and TPR for every beat from the signal of RR interval.

Step 7: Check if all the 3 parameters cross the threshold level or not. If the 3 parameters cross the threshold level then return 1 else 0, 1 represents AF and 0 represents NSR.

Step 8: Compare the results with the annotation files provided in the MIT-BIH database and calculate the number of TP, TN, FP and FN.

Step 9: From the number of TP, TN, FP and FN calculate the sensitivity, specificity and accuracy.

4.2.3 Detection Methods

Recently different mathematical models and statistical models are used for early AF detection [4.14]. It already established that RR-intervals would be used for the detection method. The irregularity and variability are the main characteristics for AF [4.14]. In this thesis, we use statistical analysis to distinguish between the degrees of variability. Three different statistical methods were followed throughout the thesis. Those methods were root mean squares of successive differences (RMSSD), Shannon entropy (SE) and turning point ratio (TPR). RMSSD is a statistical parameter that measures the variability within a data set. SE is a statistical parameter that measures the uncertainty of a random variable. TPR is a statistic that measures the random fluctuations within a data set.

The algorithm that is used for this thesis is based on the increased variability and complexity in the RR intervals series due to the atrial fibrillation. In this algorithm, each series of RR intervals was divided into 128 overlapping beat segments. Every set of beat segment began 1 RR interval after the beginning of previous set of beat segment. Then the three statistical methods used for the analysis whether each 128-beat segment contains the characteristics of AF or not. Among the three tests RMSSD and SE are parametric test, and TPR is a non-

parametric test. Here the two parametric tests were affected by distribution assumptions. So, from each 128-beat segment the shortest 8 beats and the longest 8 beats were removed. Each set of 128 beat segments was flagged as AF if all the three statistical methods determined it to be AF.

Root Mean Squares of Successive Differences (RMSSD): RMSSD is a statistical parameter that is used to measure the variability within a data set. It is one of the few time domain tools that is used to measure heart rate variability (HRV). As the RMSSD is a parametric test it is sensitive to the outlier. So, the shortest 8 and longest 8 RR intervals is actually the sum of the squares of each difference between each consecutive RR intervals. So, the expression of RMSSD that is used in our algorithm is [4.15],

$$RMSSD = \sqrt{\frac{1}{l-1} \times \sum_{i=1}^{l-1} (rr_{i+1} - rr_i)^2}$$

For compensating with the changes in the heart rate overtime and also the premature ventricular contractions RMSSD was divided by the mean RR value of each segment. In this algorithm $RMSSD/(\text{mean RR}) > 0.1$ was selected as the threshold for AF detection [4.15].

Shannon Entropy (SE): SE is a statistical parameter that is used for the measurement of the uncertainty of random variable. SE is also a parametric test that is sensitive to outlier. So as we do in the case of RMSSD, we have to remove the shortest 8 and longest 8 RR intervals. SE is a parameter that measures the complexity of a data set and the ability to predict future data point from past data point. The higher the value of SE represents higher uncertainty of the random variable. The lower value of SE represents lower uncertainty of the random variable. In this algorithm, it is associated that SE will be higher than the Normal Sinus Rhythm (NSR). After removing the 8 longest and 8 shortest outliers a histogram was constructed with 16 equally spaced bins using the remaining data points in each 128 beat segment. Using 16 bins was found to provide sufficient resolution. Too many bins will result in a significant distortion. The value of SE approaches to zero if the number of bins approaches to infinity. Then the number of RR interval in each was computed. The probability for each bin is computed as [4.15],

$$p(i) = \frac{N_i}{1 - N_{\text{Outliers}}}$$

Where, N_i = the number of beats in a particular bin,

l = the segment length,

N_{Outliers} = the number of outliers.

Then SE is [4.15],

$$SE = \sum_{i=1}^{16} p(i) \frac{\log(p(i))}{\log(\frac{1}{16})}$$

In this thesis we selected $SE > 0.7$ as the threshold for AF detection [4.15].

Turning Point Ratio (TPR): TPR is a non-parametric statistic that is used to measure the degree of randomness in a particular time series. Turning points are the points which are greater than or less than both the succeeding and preceding terms. TPR compares the amount of turning points in each set of data and to the maximum number of possible turning points. Each beat in RR irregularity (RRI) segment compared to its 2 nearest neighbors is designated a turning point if it is greater than or lesser than both [4.15]. That statistical test that use in this algorithm is if the sequence is stationary then the RR intervals are random which corresponds to AF. And if the sequence is non-stationary then the RR intervals are non-random corresponds to normal sinus rhythm. For random data points of arbitrary length (l) the expected number of turning point is [4.15],

$$\mu_{\text{TP}} = \frac{(2l - 4)}{3}$$

And with a standard deviation of [4.15],

$$\sigma_{\text{TP}} = \sqrt{\frac{(16l - 29)}{90}}$$

If any data does not exhibit random behavior will have a TPR significantly greater than or less than the expected value of 0.66. In proposed algorithm, the interval which corresponds to a TPR of $\mu \pm 3.2\sigma$ was marked as AF. For the selected beat segment length of 128, $0.54 < \text{TPR} < 0.77$ will be marked as AF [4.15].

4.2.4 Performance Criteria

In this chapter, three performance criteria used such as sensitivity, specificity, accuracy to verify the results of proposed algorithm. To test those performance criteria, the MIT-BIH Atrial Fibrillation database [4.16] is used from where we take the ECG signal. Beside the main ECG signal the database also contains annotation files. Those annotation files contain the information of each beat whether it has AF or not. Then that information is compared with simulation results of proposed work. Each beat is annotated with 1 for AF and 0 for Normal Sinus Rhythm (NSR). In proposed algorithm used 1 for AF and 0 for NSR. The result of any segment is counted as the result of the first beat of that segment. After the comparison, we separated the beats into four categories. They are True Positive (TP), True Negative (TN), False Positive (FP) and False Negative (FN). TP beats are those beats that annotated as 1 in both the database and in the result. TN beats are those beats that annotated as 0 in the database and also in the result. FP beats are those beats that is annotated as 0 in the database but annotated as 1 in the result. FN beats are those beats that is annotated as 1 in the database but annotated as 0 in the result. The number of TP, TN, FP, and FN are used to calculate the three performance criteria of the algorithm, like:

$$\text{Sensitivity} = \frac{(\text{Number of true positive assessment})}{(\text{Number of all positive assessment})} = \frac{\text{TP}}{(\text{TP} + \text{FN})}$$

$$\text{Specificity} = \frac{(\text{Number of true negative assessment})}{(\text{Number of all negative assessment})} = \frac{\text{TN}}{(\text{TN} + \text{FP})}$$

$$\text{Accuracy} = \frac{(\text{Number of correct assessments})}{(\text{Number of all assessments})} = \frac{(\text{TN} + \text{TP})}{(\text{TN} + \text{TP} + \text{FN} + \text{FP})}$$

4.3 Results and Discussion

The results and discussion of proposed algorithm are described in details in some subsections bellows:

4.3.1 Import of ECG Signal

At first, we have to take an input ECG signal for analysis in MATLAB environment. As mentioned before, we import ECG signals from the MIT-BIH Atrial Fibrillation database [4.16]. The signals that are stored in the database are in .qrs and .dat format. This is

digitalized format. For simplicity, we transform the data into .mat format so that it can be easily loaded into MATLAB. Then, it is represented in the time domain as shown in Figure 4.2. The data are sampled at 250 times per second.

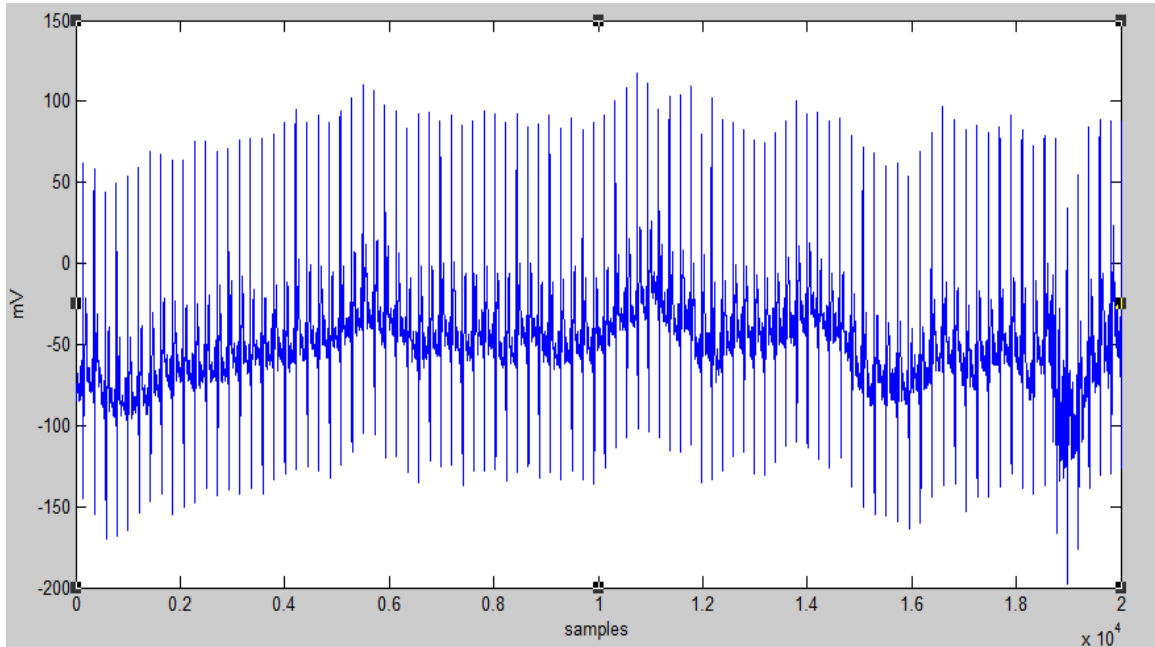


Figure 4. 2: Time domain representation of original ECG signal (File # 04048).

4.3.2 Filtering of Baseline Noise of ECG Signal

To reach our main objective we have to detect the R-peaks of the signal. The signals that are stored in the MIT-BIH Atrial Fibrillation database usually have some baseline noise that shifts the baseline of the ECG signals. This happens because of the patient's physical condition, state, movement and other criteria. So, to define the threshold level for the R peak we have to remove the noise. We use the multistage multirate system (case III) for filtering the signal. After filtering we represent the filtered signal to time domain, as shown in Figure 4.3.

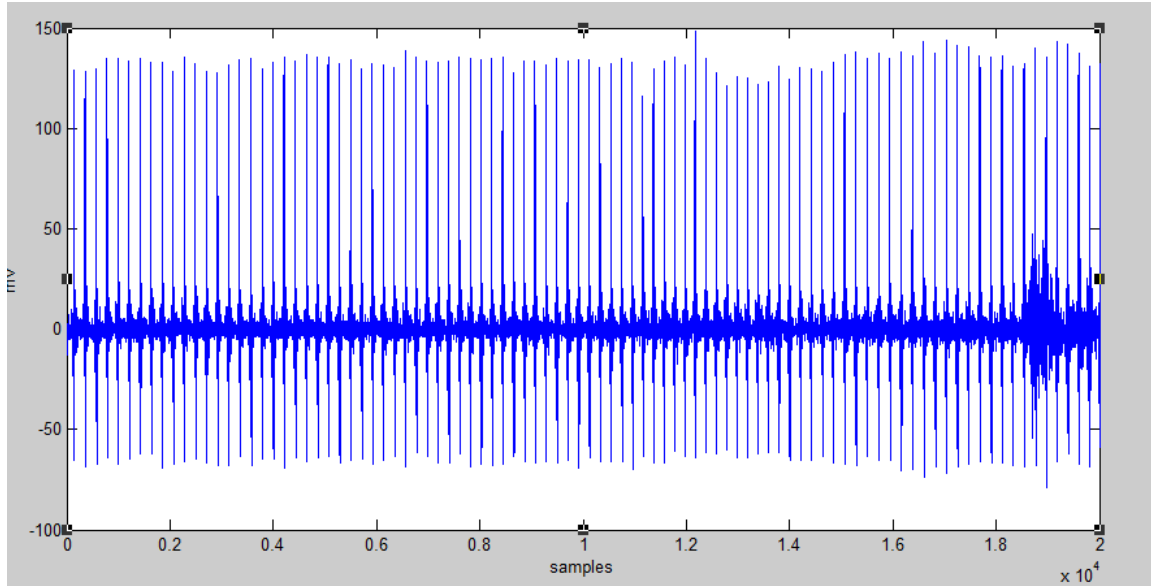


Figure 4. 3: Time domain representation of filtered ECG (File # 04048).

4.3.3 R-R peak detection

After filtering the signal we can easily define the threshold of the filtered signal for detecting the R wave peaks. By observing the Figure 4.3, 95 is defined as the threshold of the signal because it is clearly seen that the amplitude of all the R peaks are above 95. The detected R peaks are shown in Figure 4.4.

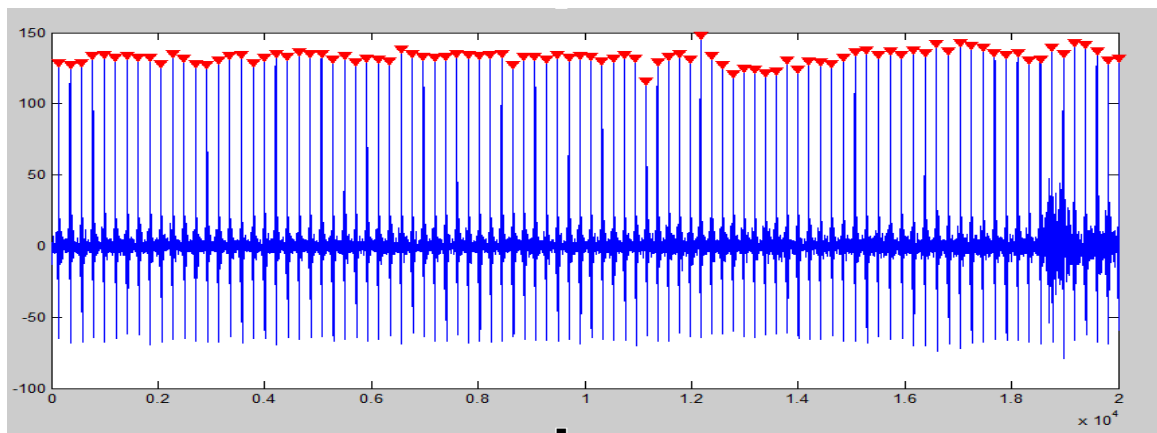


Figure 4. 4: R peak detection of the filtered ECG signal (File # 04048).

Due to the variability of amplitudes of the signals that provided in the MIH-BIH Atrial Fibrillation database, we have to select different threshold level for different signals. We observed 15 original ECG signals recorded in the database. The threshold levels for those signals are given below in Table 4.1.

Table 4. 1: Threshold levels of 15 original ECG signals recorded in MIT-BIH Atrial Fibrillation database [4.16].

Sl. No.	Original ECG Signal (File #)	Threshold level
1	04015	192
2	04048	95
3	04126	107
4	04746	171
5	04908	176
6	05121	152
7	05261	121
8	06426	277
9	06995	132
10	07162	26
11	07859	18
12	07879	112
13	07910	131
14	08215	71
15	08219	117

4.3.4 Signal for RR Peak Differences

After finding the R peaks we have to calculate the difference between each successive R peaks. Then we plot the RR interval against each beat, as shown in Fig. 4.5. This signal is required to detect AF.

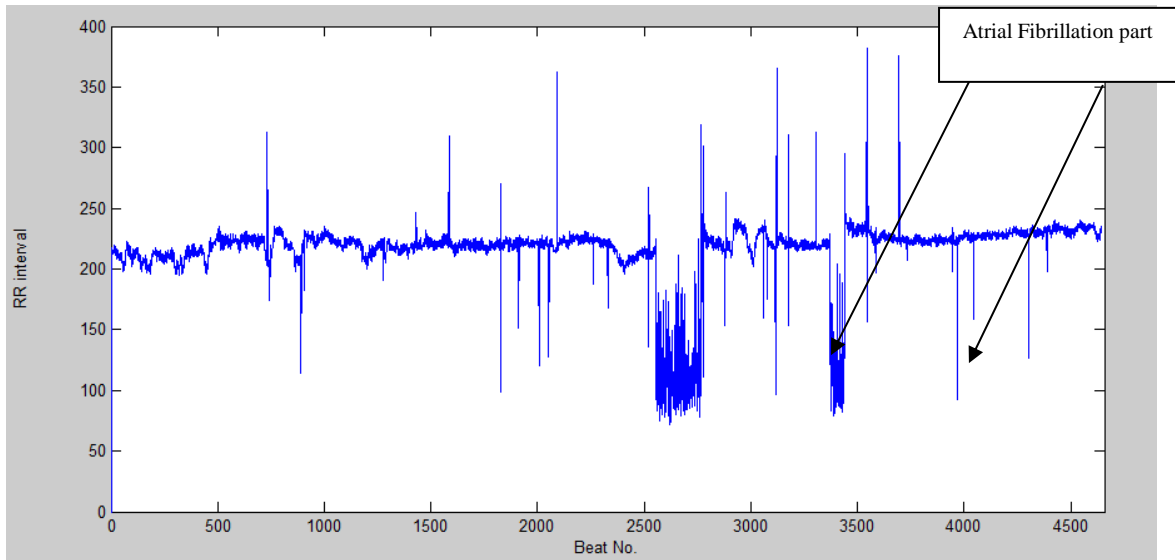


Figure 4. 5: Wave shapes of RR interval of the signal (File # 04048).

4.3.5 AF Detection Results

After getting the signal of RR intervals we calculate RMSSD, SE and TPR for every single beat. In case of RMSSD and SE, we consider 128 beat as a data set to calculate RMSSD and SE. The resultant RMSSD and SE is considered as the RMSSD and SE of the first beat. The results of RMSSD, SE and TPR for File # 04048 are showed in Figures 4.6-4.8 respectively, so that, we could compare it with Figure 4.5.

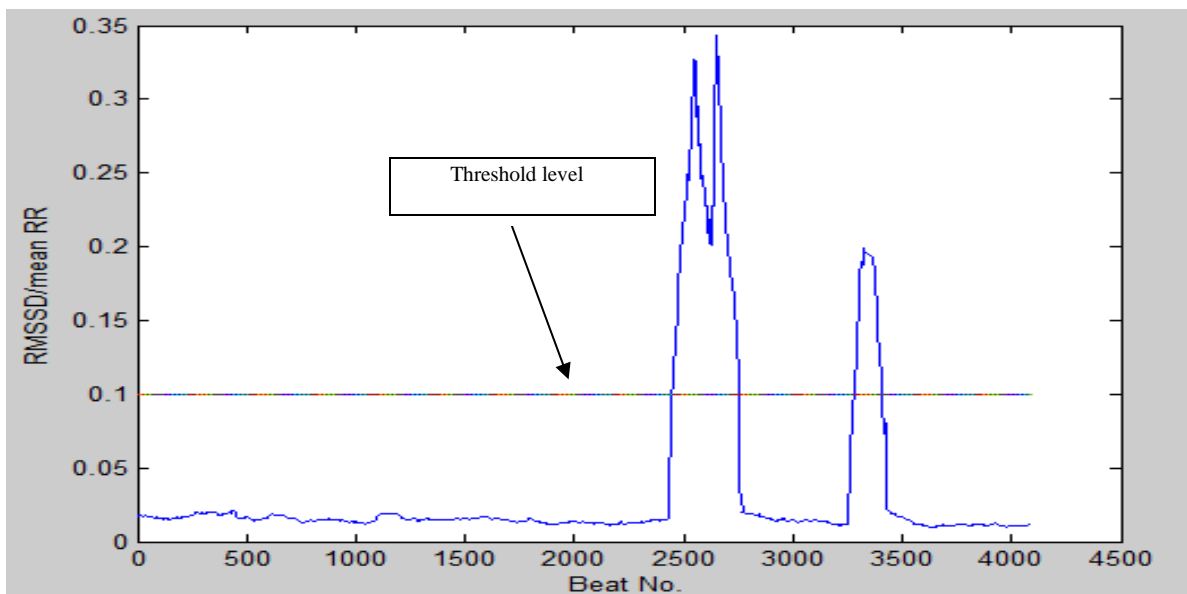


Figure 4. 6: Result of RMSSD of the signal (File #04048).

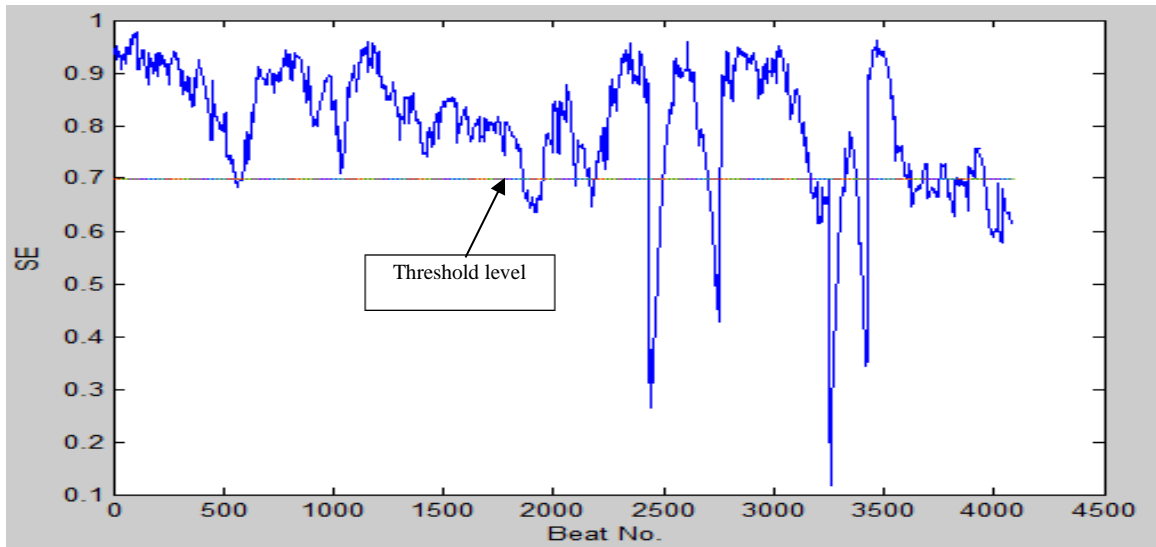


Figure 4. 7: Result of SE of the signal (File #04048).

In proposed algorithm we use the threshold level of RMSSD/ (mean RR) is 0.1 [4.15]. By comparing Figure 4.5 and Figure 4.6 it is clearly seen that the threshold level of RMSSD is able to detect most of the AF beats.

In proposed algorithm we use the threshold level of SE is 0.8 [4.15]. By comparing Figure 4.5 and Figure 4.7 it is clearly seen that the threshold level of SE is able to detect most of the AF beats.

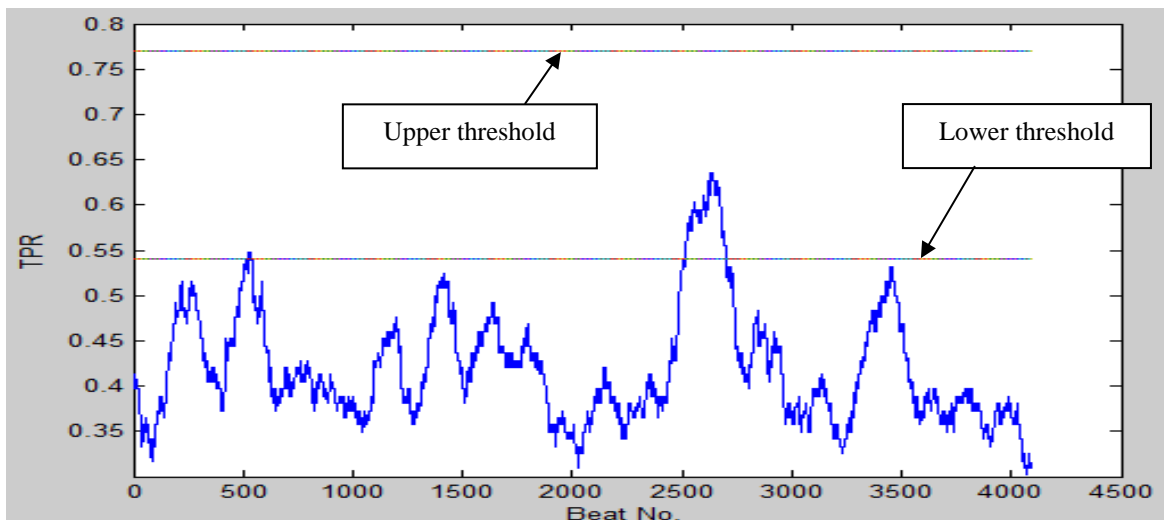


Figure 4. 8: Result of TPR of the signal (File #04048).

Table 4. 2: Number of NSR and AF detected in our algorithm.

Sl. No.	Original ECG Signal (File #)	Total No. of Beats	Result of Algorithm		Annotation results provided in database	
			Number of NSR	Number of AF	Number of NSR	Number of AF
1	04015	43288	42779	509	42794	494
2	04048	40163	39514	649	39517	646
3	04126	43507	39995	3512	40018	3489
4	04746	48789	17835	30954	17885	30904
5	04908	62090	55618	6472	55719	6371
6	05121	57522	19424	38098	19639	37883
7	05261	48514	43388	5126	43455	5059
8	06426	55489	3799	51690	3934	51555
9	06995	55142	29008	26134	29375	25767
10	07162	44435	90	44345	0	44435
11	07859	64516	147	64369	0	64516
12	07879	56878	16241	40637	16780	40098
13	07910	36198	29522	6676	29720	6478
14	08215	59710	14792	44918	14971	44739
15	08219	59177	48665	10512	48714	10463

In proposed algorithm we use the upper threshold level of TPR is 0.77 and lower Threshold of TPR is 0.54 [4.15]. By comparing Figure 4.5 and Figure 4.8 it is clearly seen that the threshold level of TPR is able to detect most of the AF beats.

In this algorithm, each beat flagged with 0 for NSR and 1 for AF. The number of NSR and AF detected in proposed algorithm is given in Table 4.2. And also, the number of NSR and

AF that provided in the database annotation files has given with it. The table 4.3 clearly shows that the number of NSR plus the number of AF obtained in proposed algorithm is equal to the total number of beats which is almost same with the annotation results provided in the database, revealing the good performance of the proposed algorithm.

4.3.6 Performance Analysis of Proposed Algorithm

In order to evaluate the performance of proposed algorithm, we calculate several performance criteria, such as, sensitivity, specificity and accuracy. To calculate those factors, at first, we have to calculate TP, TN, FP and FN. TP beats are those beats which are annotated as 1 or AF both in algorithm and database. TN beats are those beats which are annotated as 0 or NSR both in algorithm and database. FP beats are those beats which are annotated as 1 or AF in algorithm but annotated as 0 or NSR in database. FN beats are those beats which are annotated as 0 or NSR in the algorithm but annotated as 1 or AF in the database. The number of TP, TN, FP and FN for each signal is given in Table 4.3.

Table 4. 3: Number of TP, TN, FP and FN for each ECG signal.

Sl. No.	Original ECG Signal (File #)	True Positive TP	True Negative TN	False Positive FP	False Negative FN
1	04015	479	42764	30	15
2	04048	623	39491	26	23
3	04126	3459	39965	53	30
4	04746	30804	17735	150	100
5	04908	6300	55547	172	71
6	05121	37812	19353	286	71
7	05261	5032	43361	94	27
8	06426	51498	3260	92	57
9	06995	25598	28839	536	169
10	07162	44345	0	0	90
11	07859	64369	0	0	147
12	07879	40057	16200	580	41
13	07910	6384	29428	292	94
14	08215	44594	14647	324	145
15	08219	10092	48294	420	371

Table 4. 4: The calculated value of sensitivity, specificity and accuracy of the tested data.

Sl. No.	Original ECG Signal (File #)	Sensitivity (%)	Specificity (%)	Accuracy (%)
1	04015	96.96	99.93	99.89
2	04048	96.43	99.90	99.94
3	04126	99.14	99.86	99.87
4	04746	99.69	99.16	99.67
5	04908	98.88	97.69	99.60
6	05121	99.81	98.54	99.37
7	05261	99.47	99.78	99.75
8	06426	99.88	94.43	98.68
9	06995	99.34	98.17	98.72
10	07162	99.78	100	99.80
11	07859	99.77	100	99.77
12	07879	99.89	98.54	98.91
13	07910	99.55	99.02	98.93
14	08215	99.68	98.84	99.21
15	08219	97.45	99.13	98.67

From the data provided in the Table 4.3, we can easily calculate the sensitivity, specificity and accuracy of the algorithm. Sensitivity is the ability of the algorithm to detect the AF beats. Specificity is the ability of the algorithm to detect NSR. Accuracy is the overall detection ability of the algorithm. The calculated values of sensitivity, specificity and accuracy of each signal is given in Table 4.4.

From the Table 4.4 it is seen that in most of the cases proposed algorithm has a very high sensitivity, specificity and accuracy. Also from the data given in the Table 4.4 we were able to calculate the weighted values of sensitivity, specificity and accuracy, and the values are given Table 4.5.

Table 4. 5: The weighted value of sensitivity, specificity and accuracy of the tested data.

Original ECG signal (file #)	Sensitivity	Specificity	Accuracy	Size	Total Size	Total Weight	Weighted Sensitivity	Weighted Specificity	Weighted Accuracy
04015	.9989	.9993	.9696	43288	775418	.05583	.0558	.0558	.0541
04048	.9994	.9993	.9643	40163	775418	.05179	.0518	.0518	.0499
04126	.9987	.9986	.9914	43507	775418	.0561	.0560	.0560	.0556
04746	.9968	.9916	.9969	48789	775418	.06292	.0627	.0624	.0627
04908	.9960	.9769	.9888	62090	775418	.08007	.0797	.0782	.0791
05121	.9937	.9854	.9981	57522	775418	.07418	.0737	.0730	.0746
05261	.9975	.9978	.9947	48514	775418	.06256	.0623	.0636	.0621
06426	.9868	.9443	.9988	55489	775418	.07156	.0706	.0675	.0714
06995	.9872	.9817	.9934	55142	775418	.07111	.0701	.0698	.0706
07162	.9980	1	.9978	44435	775418	.0573	.0572	.0573	.0572
07859	.9977	1	.9977	64516	775418	.0832	.0830	.0832	.0830
07879	.9891	.9854	.9989	56878	775418	.07335	.0726	.0723	.0733
07910	.9895	.9902	.9954	36189	775418	.0467	.0462	.0462	.0465
08215	.9921	.9884	.9968	59710	775418	.0770	.0764	.0761	.0768
08219	.9867	.9913	.9745	59177	775418	.0763	.0753	.0756	.0744
							98.03%	98.80%	99.45%

The table 4.5 clearly shows that the average value of the weighted sensitivity, specificity and accuracy are over 98.03%, 98.80%, and 99.45% respectively which is very much compatible with the other results found in literature [4.5-4.9, 4.17-4.20]. This indicates that the algorithm or technique used in this work is suited for detecting AF using ECG signal.

In this chapter we use the algorithm that mainly follows statistical method for detection AF. Using proposed algorithm, we achieved the results such as sensitivity of 98.03%, specificity of 98.80% and accuracy of 99.45% which makes the algorithm clinically applicable for AF detection. As it follows the RRI method, it is much easier and simpler. If this algorithm is implemented practically into diagnostic test, it could reduce cost allow doctors to detect AF before the condition of the patients are at high risk for complications such as stroke and heart attack.

4.4 Summary

The algorithm that is used in this chapter is able to detect the AF with high degree of accuracy. It is seen that this algorithm has higher degree in sensitivity specificity and accuracy. The MIT BIH Atrial Fibrillation database is used to import ECG data for analysis. RR interval of the ECG signal is calculated. We are used the algorithm that mainly follows statistical method for detection of AF. Parametric statistic RMSSD and SE, and non-parametric statistic, TPR are used for this purpose. The resultant value of RMSSD, SE and TPR of every beat is checked weather it crosses the threshold level or not. If all the three parameters cross the threshold level then the beat flagged as AF. It shows excellent result when compared with the annotations of the database, and then the sensitivity, specificity and accuracy is determined. The algorithm has the sensitivity of 98.03%, specificity of 98.80% and accuracy of 99.45%.

The next chapter will cover the conclusion of this thesis.

REFERENCES

- [4.1] C. Brüser, J. Diesel, M.D.H. Zink, S. Winter, P. Schauerte and S. Leonhardt, “Automatic Detection of Atrial Fibrillation in Cardiac Vibration Signals”, *IEEE J. Biomed. Health Informatics*, vol. 17, no. 1, pp. 162-171, 2013.
- [4.2] M. Keech, Y. Punekar, A. M. Choy, “Trends in Atrial Fibrillation Hospitalisation in Scotland: An Increasing cost burden”, *Br. J. Cardiol*, vol.19, pp. 173–177, 2012.
- [4.3] C.A. Sanoski and D. Pharm, “Clinical, Economic, and Quality of Life Impact of Atrial Fibrillation”, *J Manag Care Pharm*.15 (6 Suppl B):S4- 9,August 2009.
- [4.4] N. Larburu, T Lopetegi and I Romero, “Comparative Study of Algorithms for Atrial Fibrillation Detection”, *Computing in Cardiology*, Hangzhon: IEEE, vol. 1. pp. 265-268, 2011.
- [4.5] G. Moody and R. Mark, “A New Method for Detecting Atrial Fibrillation Using RR Intervals”, *Computers in Cardiology*, Aachen: *IEEE Computer Society Press*, vol. 10, pp. 227–230, 1983.
- [4.6] B. Logan and J. Healey, “Robust Detection of Atrial Fibrillation for a Long-Term Telemonitoring System”, *Computers in Cardiology*, vol. 32, pp. 619-622, 2005.
- [4.7] D. T. Linker, “Long-Term Monitoring for Detection of Atrial Fibrillation”, *Patent Application Publication*, Seattle, US, 2006.
- [4.8] K. Tateno and L. Glass, “Automatic Detection of Atrial Fibrillation Using the Coefficient of Variation and Density Histograms of RR and $_RR$ Intervals”, *Medical & Biological Engineering & Computing*, vol. 39, no. 6, pp. 664–671, 2001.
- [4.9] S. Cerutti, L. Mainardi, A. Porta and A. Bianchi, “Analysis of the Dynamics of RR Interval Series for the Detection of Atrial Fibrillation Episodes”, *Computers in Cardiology*, vol. 24, pp. 77-80, 1997.
- [4.10] R. E. Crochiere and L. R. Rabiner, “Multirate Digital Signal Processing”, Publisher: *Pearson*; *1st edition*, ISBN-13: 978-0136051626, March 21, 1983.
- [4.11] P. P. Vaidyanathan, “Multirate System and Filter Banks”, Publisher: *Prentice Hall*; *1 edition*, ISBN-13: 978-0136057185, October 1, 1992.
- [4.12] R.G. Shenoy, D. Burnside and T.W. Parks, “Linear Periodic Systems and Multirate Filter Design”, *IEEE Transactions on Signal Processing*, vol. 42, Issue: 9, pp.2242 – 2256, September 1994.

- [4.13] G. A. Williamson, S. Dasgupta and F. Minyue, “Multistage Multirate Adaptive Filters”, *IEEE International Conference on Acoustic, Speech, and Signal Processing conference Proceedings*, vol. 3, pp. 1534–1537, 1999.
- [4.14] S. Hargittai, “Is it Possible to Detect Atrial Fibrillation by Simply using RR Intervals?”, *Computers in Cardiology*, vol. 41, pp. 897-900, 2014.
- [4.15] S. Dash, E. Raeder, S. Merchant and K. Chon, “A Statistical Approach for Accurate Detection of Atrial Fibrillation and Flutter”, *Computers in Cardiology*, vol. 36, pp. 137-140, 2009.
- [4.16] MIT-BIH Atrial Fibrillation Database, Online Available: <http://physionet.org/physiobank/database/afdb>, 2014.
- [4.17] J. Slocum, A. Sahakian and S. Swiryn, “Diagnosis of Atrial Fibrillation from Surface Electrocardiograms Based on Computer-detected Atrial Activity”, *Journal of Electrocardiology*, vol. 25, pp. 1-8, 1992.
- [4.18] R. Schmidt, M. Harris, D. Novac and M. Perkhun, “Atrial Fibrillation Detection”, *Patent Cooperation Treaty*, Eindhoven, Netherlands, 2008.
- [4.19] S. Babaeizadeh, R. E. Gregg, E. D. Helfenbein, J. M. Lindauer and S. H. Zhou, “Improvements in Atrial Fibrillation Detection for Real-time Monitoring”, *Journal of Electrocardiology*, Vol. 42, pp. 522-526, 2009.
- [4.20] R. Couceiro, P. Carvalho, J. Henriques, M. Antunes, M. Harris and J. Habetha, “Detection of Atrial Fibrillation Using Model-based ECG Analysis”, *19th International Conference on Pattern Recognition*, Tampa, FL, pp. 1-5, 2008.

CHAPTER V

Conclusion and Future Work

Chapter Outlines

- Conclusion
- Future Work

Chapter V

Conclusion and Future Work

5.1 Conclusion

We have successfully filtered ECG signal using multistage multirate system and also detected the RRI in ECG signal. The simulation results have shown that proposed de-noising algorithms are better for diagnostics purposes of ECG and proposed AF detection algorithm are more efficient for detection of heart diseases.

This algorithm is able to detect the AF with high degree of accuracy, comparing with other algorithms that are commonly used for AF detection, it is seen that, this algorithm has higher degree in both sensitivity and specificity. This algorithm is implemented successfully in MATLAB and able to detect AF with a fast run time, low sensitivity to noise, high accuracy and simple user interface. This algorithm is experienced over 15 ECG signals provided in the MIT-BIH Atrial Fibrillation database and achieved a sensitivity of 98.03%, specificity of 98.80% and accuracy of 99.45%.

5.2 Future Work

In this thesis work an approach is to detect AF using ECG signal by multistage multirate systems. The future work is to detect VF, AFL using ECG signal.